Department of Geodetic Science

BASIC RESEARCH AND DATA ANALYSIS FOR THE NATIONAL GEODETIC SATELLITE PROGRAM

Eighth Semiannual Status Report

Period Covered: January 1971 — June 1971
Research Grant No. NGL 36-008-093
OSURF Project No. 2514

Prepared for
National Aeronautics and Space Administration
Washington, D.C. 20546

The Ohio State University
Research Foundation
Columbus, Ohio 43212
July 1971

PREFACE

This project is under the supervision of Professor Ivan I. Mueller, Department of Geodetic Science, OSU, and it is under the technical direction of Mr. Jerome D. Rosenberg, Deputy Director, Communications Programs, OSSA, NASA Headquarters, Washington, D. C. The contract is administered by the Office of University Affairs, NASA, Washington, D. C. 20546.

TABLE OF CONTENTS

LIST OF FIGURES

LIST OF TABLES

1. STATEMENT OF WORK

The statement of work for this project includes data analysis and supporting research in connection with the following broad objectives:

(1) Provide a precise and accurate geometric description of the earth's surface.

(2) Provide a precise and accurate mathematical description of earth's gravitational field.

(3) Determine time variations of the geometry of the ocean surface, the solid earth, the gravity field, and other geophysical parameters.

2. ACCOMPLISHMENTS DURING THE REPORT PERIOD

2.1 Gravity Field Refinement by Satellite to Satellite Doppler Tracking

2.11 Introduction.

Almost all of our present knowledge about the broad scale features of the gravity field (i.e. those features described by spherical harmonics of low degree and order) has been obtained from satellite gravimetry. The main advantage of using the motion of artificial satellites to determine the earth's gravity field is that the satellites can sample the gravity field on a global basis, thus largely avoiding sample biases due to incomplete coverage of the earth's surface. The main disadvantage is that the magnitudes of the perturbing effects of low degree terms in the geopotential fall off with increasing altitude, so that it is difficult to separate the many small perturbations from normal satellite altitudes. Using very low satellites would largely circumvent this difficulty; however, very low satellites are greatly perturbed by the retarding effect of the earth's upper atmosphere, and also require a fairly dense network of ground tracking stations to monitor their motion.

The precision of ground based tracking of artificial satellites has greatly increased since satellites were first tracked for geodetic purposes. The most promising systems being developed today are the pulsed laser systems. However, the ultimate accuracy of the laser systems is limited by the uncertainty of the tropospheric refraction correction.

This ultimate limitation in the accuracy of laser ranging will not allow the determination of terms in the geopotential above degree 22 or so with the present satellites that are equipped with laser retroreflectors [Gaposchkin, 1970]. Classical ground based gravimetry can resolve local features in the gravity field that are several kilometers or tens of kilometers in extent. However, this method

cannot satisfactorily survey features many hundreds or thousands of kilometers in extent; nor can it satisfactorily survey the gravity field on a global basis to determine the spectral components of the gravity field. If satellite gravimetry is to fill in the gap between our present knowledge of the harmonic expansion of the gravity field and the kind of information obtained by classical gravimetry, it will be necessary to use both lower satellites and new modes of satellite tracking.

One of the new methods of satellite tracking currently being discussed is satellite to satellite tracking, or using one satellite to track another. Although one satellite could conceivably track another by any of the methods that have been used for tracking of satellites from the ground, the preferred system is one using the Doppler shift of a radio signal to measure the rate of change of the range between the two satellites. Optical tracking systems have the great disadvantage that they must be precisely pointed; a Doppler measuring system is preferred over a range measuring system because the Doppler shift can be averaged over a time interval of several seconds, thus producing greater accuracy in the measurement.

There are two important advantages to using one satellite to track another. First, tracking measurements can be made on a global basis without dependence on the location of ground tracking stations. Second, the measured radio signal does not pass through the troposphere, thus circumventing the limitation imposed on ground based measurements by the indeterminancy of the tropospheric refraction correction. It has been estimated that an accuracy of 0.3 to 1.0 mm/sec in range rate measurements could be obtained with present technology, with an accuracy of 0.03 to 0.05 mm/sec eventually being possible [Kaula, 1969].

Two essentially different concepts of satellite to satellite tracking have been proposed. The first, proposed by Wolff [1969], envisages two satellites in the same low orbit, one behind the other by about 200 km. Disturbances in the gravity field along the orbital path are reflected as variations in the range rate between the two satellites. The other concept was described at the 1969 Williamstown Conference of Solid Earth and Ocean Physics [Kaula, 1969]. This concept envis-

ages a single low satellite which may be tracked by any of a constellation of very high geostationary satellites. Since the very high satellites are stationary with respect to the earth, their positions may be monitored with fixed direction antennae. Furthermore, since the high satellites will be continuously visible at the monitoring stations, the Doppler measurements may be immediately relayed to the ground, thus avoiding the need for data storage and later readout from the satellite.

The main purpose of the investigations described in this paper were to determine to what extent our knowledge of the gravity field might be refined by satellite to satellite Doppler tracking. The tool used to make this determination was a series of least squares adjustments of simulated satellite to satellite range rate observations. The unknowns in these adjustments were the orbit elements for each pass, and a set of parameters describing the gravity field.

The gravity field was represented by the density of a fictitious layer spread on the surface of the earth. This is a local representation of the gravity field, in the sense that each parameter is associated with a specific geographical area. As such, it is an appropriate representation to use when data is available to describe the gravity field only over certain portions of the earth's surface, in the same way that gravity anomalies are a more appropriate representation than a spherical harmonic series when the available data does not cover the whole surface of the earth. In fact, the properties of the surface layer representation are very similar to those of the representation by gravity anomalies, and the surface layer representation was chosen only because it is computationally more convenient for the integration of orbits than the gravity anomaly representation.

The density of surface layer was assumed to be constant in blocks of certain sizes, such as $5^\circ \times 5^\circ$ blocks, in the same way in which mean gravity anomalies in blocks are used. Many adjustments were performed, solving for the mean densities in sets of fewer than 100 blocks. Data was generated using a set of short arcs passing over the blocks in which the mean density of the surface layer was unknown. For each adjustment, the pertinent questions were 1) is the given set of data capable of determining the mean density in a block with an uncertainty which is less than the rms mean density; and 2) is the given set of data capable of satis-

factorily separating the mean density in one block from the mean densities in neighboring blocks. This latter question was answered by examining the correlation coefficients associated with the adjusted parameters.

2.12 The Range Rate Between Two Satellites Close Together in Low Orbits

Before seeing how satellite to satellite tracking can resolve the gravity field in various sized blocks, it is instructive to look at the behavior of the range rate between two satellites close together in the same low orbit. An extremely simplified situation was simulated for this purpose. The force field of the earth was represented as a dominant central force plus the attraction of a single point mass placed on the surface of the earth in the plane of the equator. The mass assigned to this point mass was 10^{-6} earth masses. A single orbit at an altitude of 1700 km was numerically integrated in this force field. The initial conditions of this orbit were chosen so that the orbit would be perfectly circular in the absence of perturbing mass. Since both the orbit and the disturbing mass lay in the equator, the situation could be viewed in two dimensions. Two satellites were assumed to be traveling in this orbit, the second passing a given point 25 seconds after the first, which corresponds to a linear separation of about 175 km.

The range rate between the two satellites for slightly over one revolution is shown in Figure 1. Two components of the range rate may be discerned. First, there is a periodic component whose period coincides with that of the orbit. This component is indicated by the dashed line. The amplitude of this component appears to increase secularly. Secondly, superimposed on the first component is a pattern which only appears when the satellite passes over the disturbing mass. This pattern can be seen clearly when the first component is subtracted from the actual range rate (Figure 2). It consists of an accelerating rise from zero to a sharp peak, followed by a fast drop to a negative extremum, followed by a return to zero. Since this pattern characterizes the range rate during the period the satellites are passing over the point mass, it may be called the characteristic signature of a point mass.

The characteristic signature shown in Figure 2 may be given an explanation that appeals to intuition by considering only the in track component of the disturbing force. As the two satellites approach the point

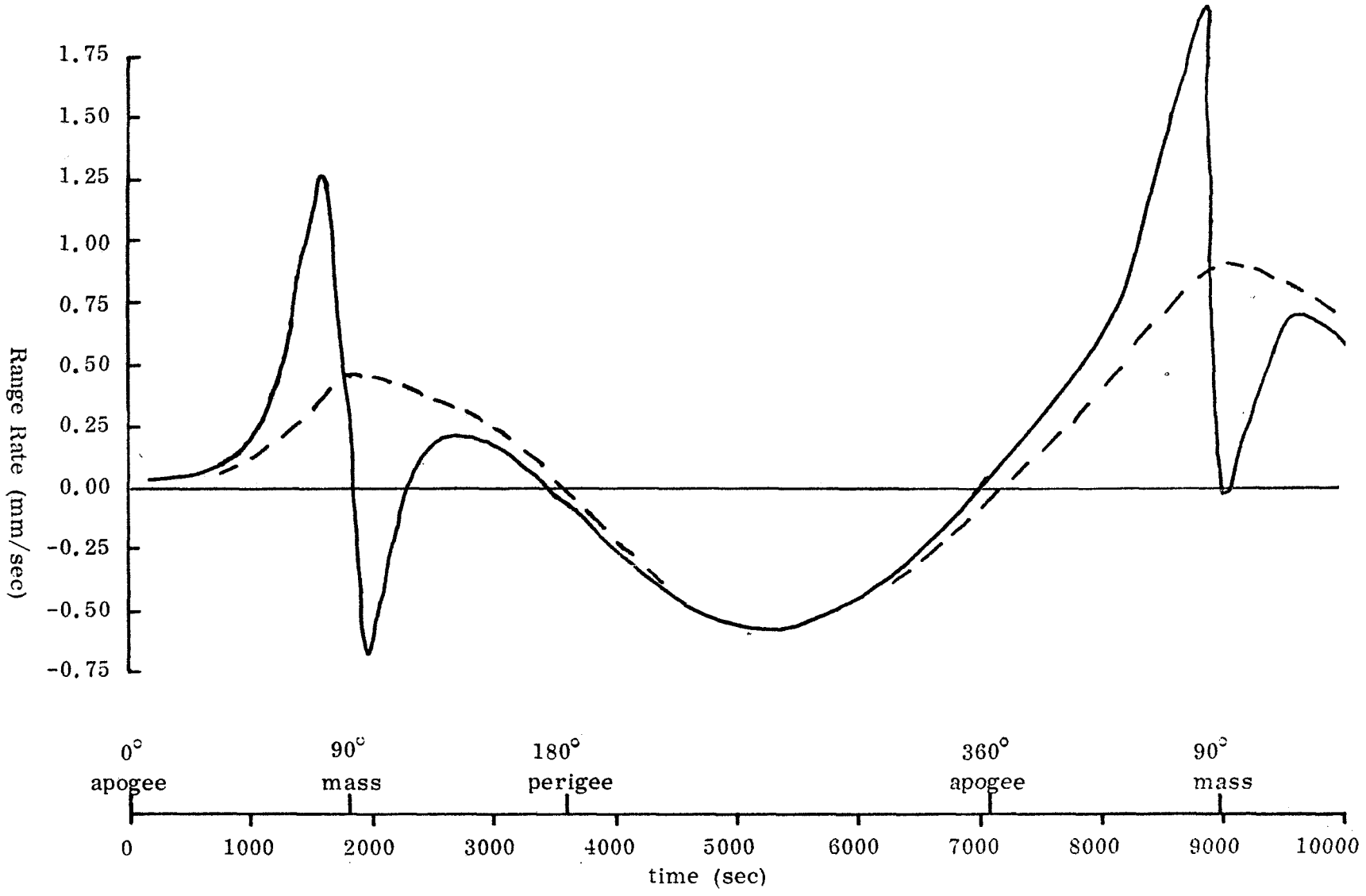

Fig. 1 . Range Rate Between Two Satellites in the Same Orbit. Dashed Line Indicates Periodic Component.

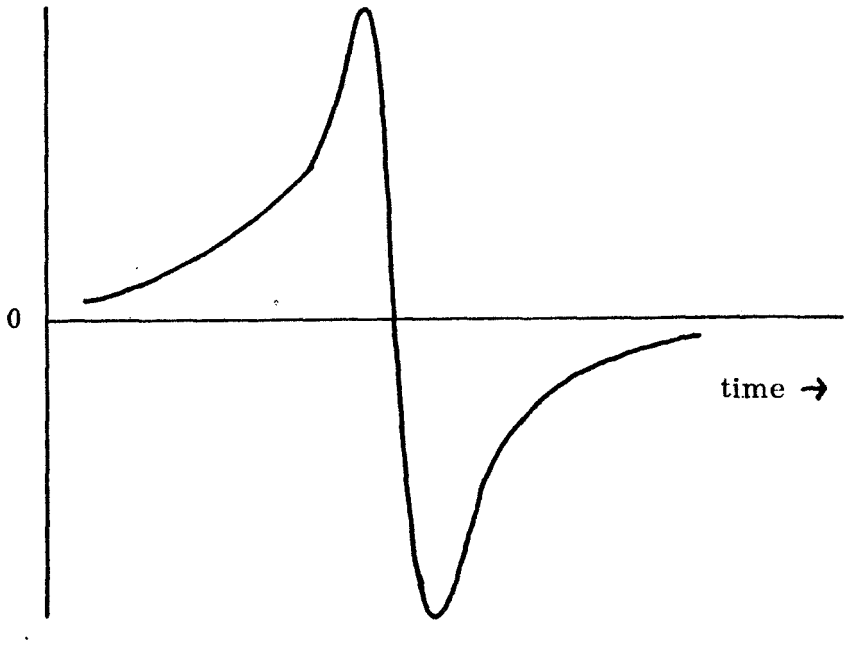

Fig. 2 Characteristic Signature of a Point Mass in the Range Rate Between Two Satellites

mass with zero relative velocity, both are attracted and the velocity of both increases. However, the first satellite, being nearer to the attracting source, is attracted more strongly. Its velocity increases faster than that of the second satellite, causing a net positive range rate as the distance between the satellites increases. The difference in the in track components of the attraction becomes more pronounced as the satellites approach the source, causing an acceleration in the graph of the range rate. When the two satellites approach within a few hundred kilometers of the attracting source, the in track components of attraction rapidly become equal again, so that the range rate reaches a maximum and ceases to increase. When the first satellite is directly over the attracting source, the horizontal component of the force with which it is attracted goes to zero; the forward velocity of the second satellite is still being increased, so the range rate between them is decreased. After the first satellite has passed the attracting source, its forward motion is retarded; the second satellite is still being attracted forward, the difference of the in track accelerations is sharply negative, and the net range rate rapidly falls to

zero and becomes negative. After the second satellite has passed several hundred kilometers beyond the attracting mass, the in track accelerations again become equal and the range rate is at a negative extremum. From that point on, the second satellite, being nearer to the attracting mass, is more strongly retarded, so that the range rate tends to increase, eventually returning to zero.

The radial component of the force exerted by the attracting mass must also be considered. The effect of this force is to pull both satellites downward, increasing their velocity and increasing the eccentricity of the orbit. Even if the initial conditions are selected so that the orbit is initially circular, the disturbing mass will cause the orbit to become eccentric. It is impossible to maintain a precisely circular orbit in the presence of disturbing forces, so that eccentricity of the orbit must be expected. The eccentricity of the orbit used to generate the range rate shown in Figure 1 was initially zero, but after one revolution, it had increased to 0.000004.

The periodic component of the range rate, on which the characteristic signature is superimposed, is caused by the eccentricity of the orbit. The growth in the amplitude of this component reflects the increasing eccentricity. Since the angular and linear velocities of the satellites are greater at perigee than at apogee, the constant time difference of 25 seconds must correspond to a larger linear separation at perigee than at apogee. This means that the separation of the two satellites must increase from apogee to perigee, as shown by a positive range rate. Similarly, the negative range rate from perigee to apogee indicates a decrease in the distance between the two satellites.

Since the total energy is constant along the orbit, the difference in gravitational potential at the positions of the two satellites is the negative of the difference in their kinetic energies. Within the small range of velocities considered, the kinetic energy difference is linearly related to the linear velocity difference, which is very nearly the range rate between the

two satellites. The difference in gravitational potential at the positions of the two satellites is shown (with the sign changed) in Figure 3. Comparison with Figure 1 shows that the difference in gravitational potential is directly proportional to the range rate.

The analysis by Wolff [1969] suggests that the range rate is also directly proportional to the rate of change of gravitational potential along the orbit, so that the actual potential may be obtained (except for a constant of integration) by integrating the range rate along the orbit. In this highly simplified example, this relationship is very nearly true. The actual gravitational potential along the orbit is shown in Figure 4. The slope of this graph is very nearly directly proportional to the potential difference in Figure 3 or to the range rate in Figure 1. The dominant component in the graph of the potential is caused by the eccentricity of the orbit, as evidenced by the minimum at apogee and the maximum at perigee. The increasing amplitude of this component reflects the increasing eccentricity. The presence of the point mass is evidenced by a small "bump" in the graph, indicating a "bump" in the gravity field.

The component due to the eccentricity may be identified by its period and removed. The remaining component contains the "bump" and approximates a profile of the gravitational potential along an arc of a circle whose radius is the mean radius of the orbit.

The relationships discussed above suggest the possibility of using many profiles to construct a contour map of the gravitational potential on a large sphere. Unfortunately these relationships can be shown to break down completely when the two satellites are in orbits that are almost, but not exactly, identical. Since it is not reasonable to expect that two satellites can be kept in precisely the same orbit, the concept of using the range rate between two orbiting satellites to map the actual potential field of the earth directly onto a sphere must be abandoned.

2.13 Assumed Gravity Fields.

Actual mean gravity anomalies in North America were used to prepare an

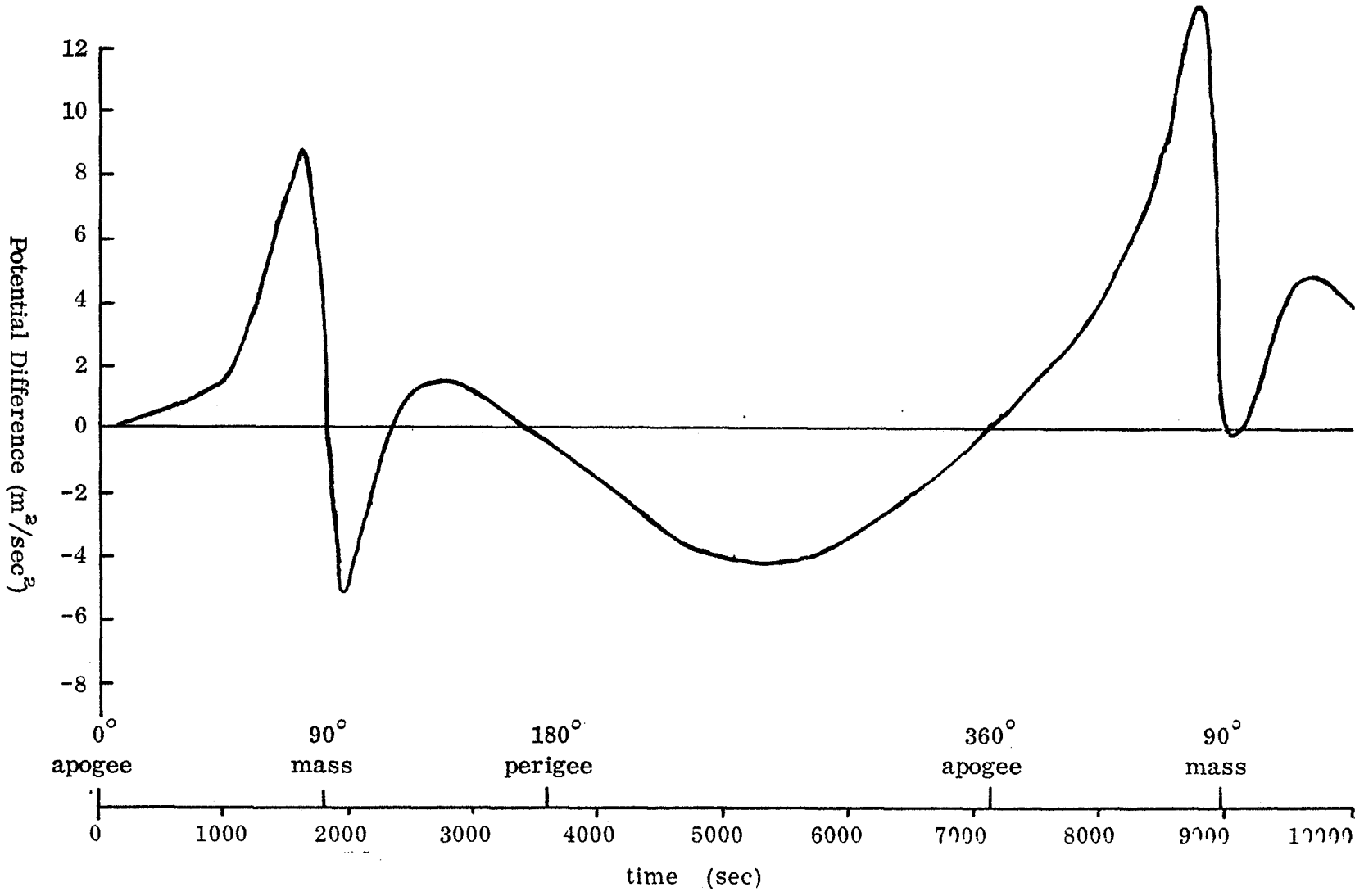

Fig. 3. Difference of Gravitational Potential for Two Satellites in the Same Orbit

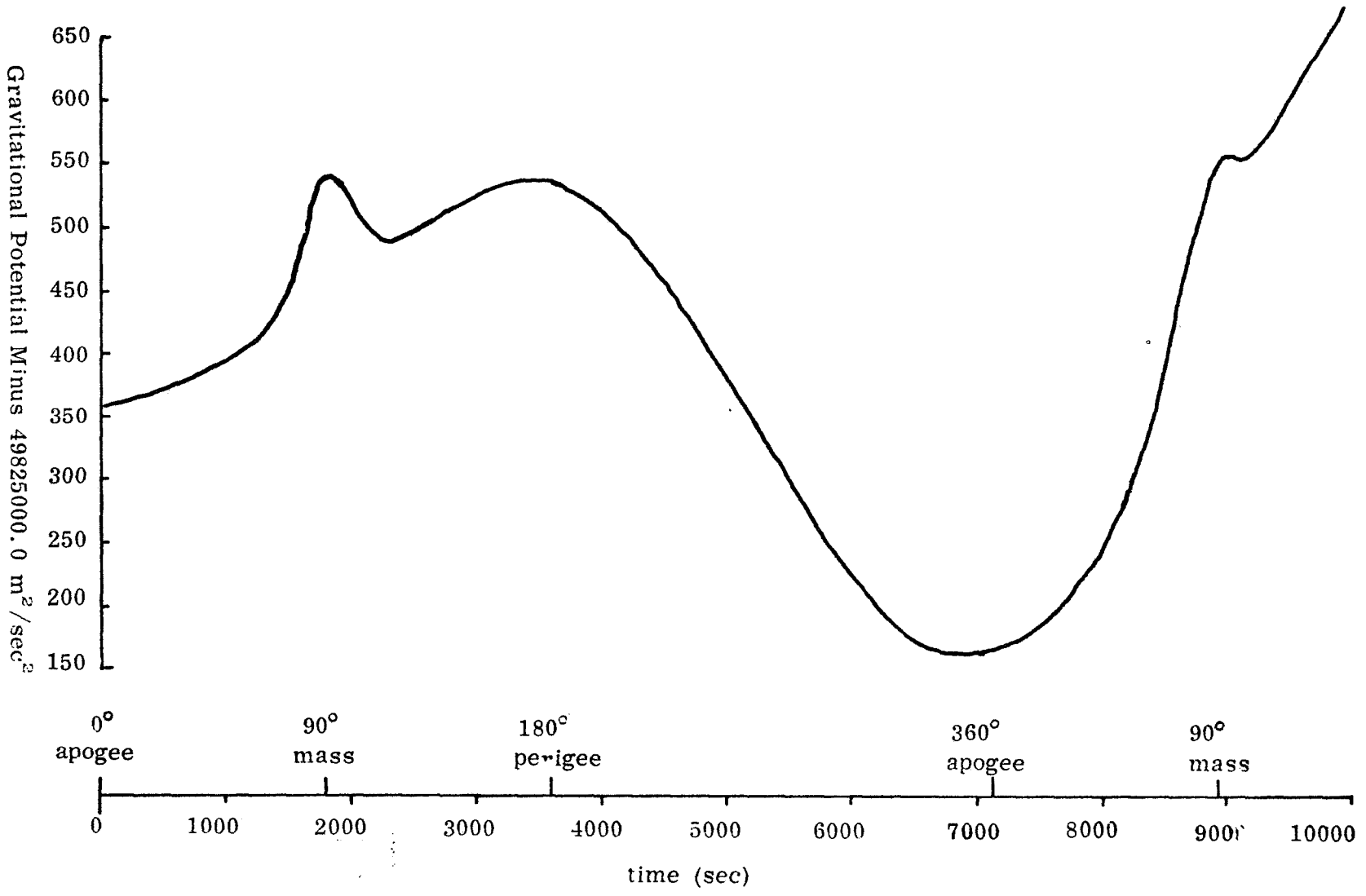

Fig. 4. Gravitational Potential Along the Orbit Perturbed by a Single Point Mass

"assumed" set of mean values of the density of the surface layer. Mean values in 92 $5^\circ \times 5^\circ$ blocks are shown in Figure 5. The density parameter φ is the product of the gravitational constant and the actual surface density. The units of the density parameter are those of acceleration, and it can be conveniently measured in milligals. The value of the density parameter is about $1/2\pi$ times that of the mean gravity anomaly in the same block. Sets of mean values of the density parameter in $2^\circ \times 2^\circ$ and $1^\circ \times 1^\circ$ blocks were also prepared. On a world wide basis, the rms mean value of the density parameter in a $5^\circ \times 5^\circ$ block is about 3.1 mgal; for a $2^\circ \times 2^\circ$ block it is about 3.9 mgal.

2.14 Sensitivity of the Range Rate to the Density of the Surface Layer

The coefficients in the observation equations describe the sensitivity of the measured quantity to each of the unknown parameters. By plotting these coefficients on a map, the effect of each block on the range rate between the two satellites may be identified. This was done for two satellites separated by 200 km in the same orbit at an altitude of 700 km. The partial derivatives with respect to the mean values of the density parameter in the 92 $5^\circ \times 5^\circ$ blocks, computed for a point near the middle of the pass, are shown in Figure 6. They describe the effect on the range rate between the satellites of a block in which the density parameter is one mgal. The sensitivity is zero in the block beneath the two satellites; it reaches a positive maximum about 700 km in front of their position, and a negative extremum about 700 km behind their position. When these sensitivities are evaluated for several points along the same orbit, the most noticeable phenomenon is that the pattern shown in Figure 6 follows the satellites along the orbit. At whatever point the partial derivatives are evaluated, an area of maximum positive sensitivity is found a short distance in front of the position of the satellites, and an area of maximum negative sensitivity is found a short distance behind their position. Furthermore, the sensitivity is zero along a line drawn midway through the satellites' positions and perpendicular to the ground path of the orbit. The sensitivities in back of this line are almost always negative and those in front of the line are positive. If the sensitivity coefficients are plotted as a function of

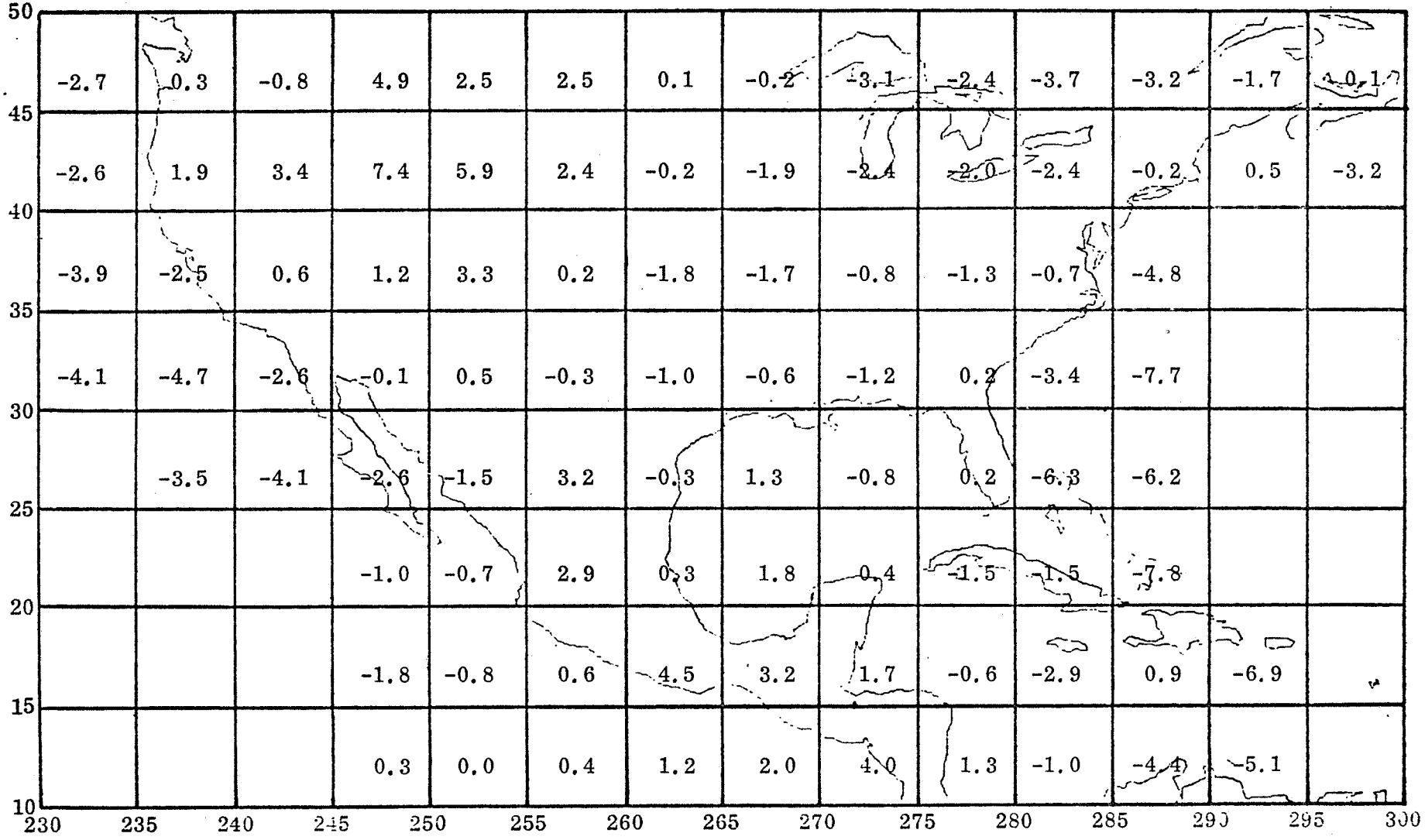

Fig. 5. $5^\circ \times 5^\circ$ Mean Values of the Density Parameter σ (mgal).

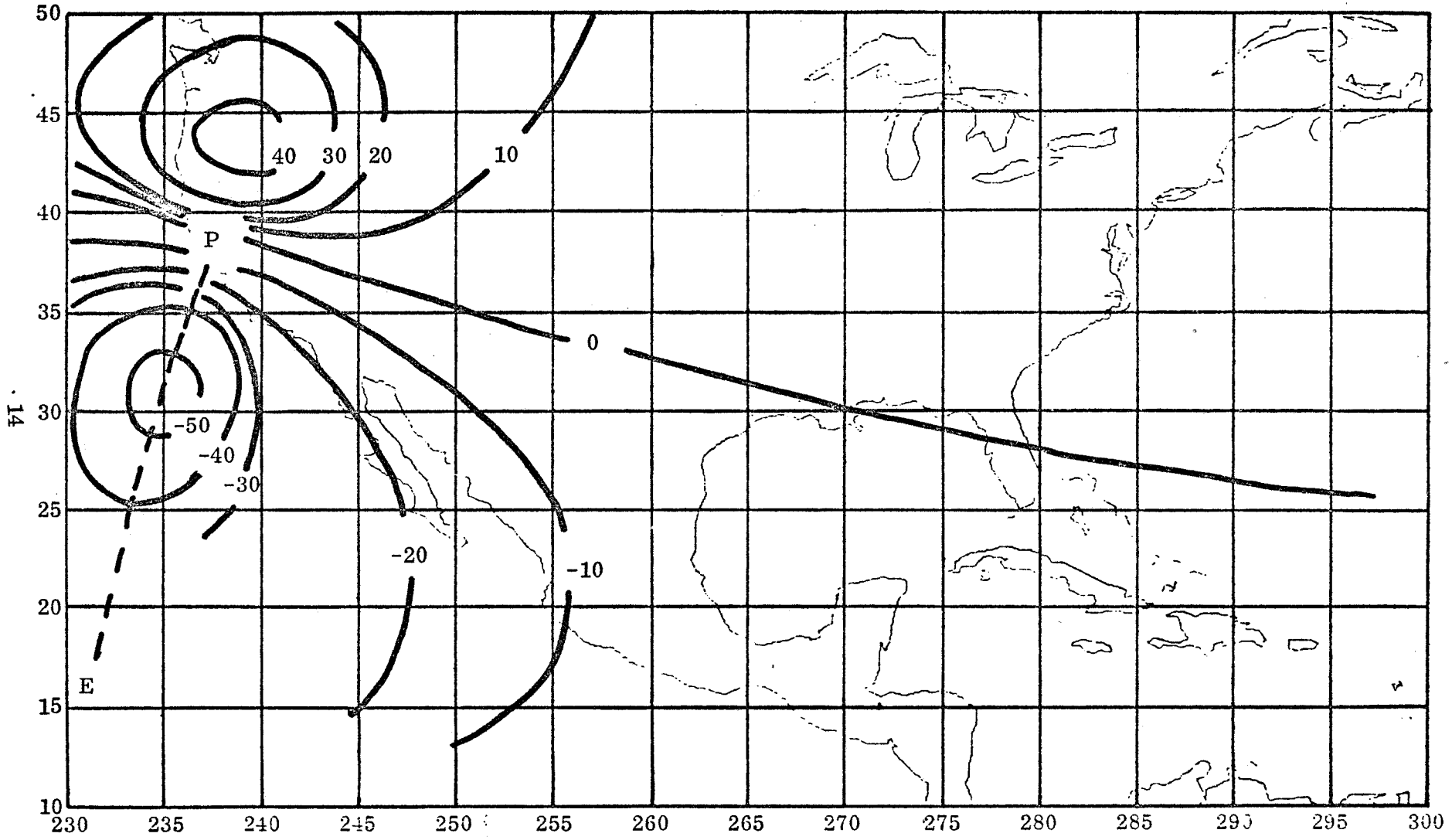

Fig. 6. Sensitivities of $\dot{\rho}$ in thousandths of a millimeter per second to φ in milligals for two satellites separated by 200 km in the same orbit 700 km high. E denotes the position at the initial epoch and P denotes the position for which the partial derivatives are evaluated.

time for a block lying on the ground path of the satellite, the typical sinusoidal signature discussed in section 2 is obtained. The effect of the surface layer in blocks far from the ground path of the orbit remain small throughout the pass. Only a few blocks have significantly large sensitivities, and among these blocks sensitivities of the range rate to the values of the parameters in two neighboring blocks are significantly different. This means that this type of observation should be well able to separate the values of the density in neighboring blocks.

For purposes of comparison, partial derivatives were also evaluated for the configuration of one low satellite tracked by a high geostationary satellite. The low satellite was in the same 700 km high orbit used for both satellites in the previous case, and the $5^\circ \times 5^\circ$ blocks were again used. The sensitivity coefficients for this case are much larger, as shown in Figure 7. In the case of two satellites in the same low orbit, the far away blocks affect both satellites in approximately the same way, and thus have little net effect on the range rate between them. While a single low satellite tracked by a high satellite approaches a block of positive density along the ground path of the orbit, the surface layer in that block continually attracts the satellite, thus increasing the velocity toward the block. After the satellite passes, it is pulled back and its velocity tends to decrease. However, the satellite has also been pulled downward into a lower orbit during the entire pass, which serves to increase its velocity. The net effect is an accumulative increase in velocity which is steepest during the time the satellite approaches the block and levels off as the satellite passes the block. However, this means that the blocks that have the greatest effect on the range rate are those far back on the ground path of the orbit, not those in the vicinity of the satellite position. Furthermore, all blocks very far back on the ground path will have approximately the same large effect on the range rate. This means that a single pass of two satellites in this configuration cannot be expected to separate the values of the density in neighboring blocks as efficiently as the two satellites in the same low orbit. On the other hand, the densities in neighboring blocks can be separated by using orbits of different inclinations, or a combination of ascending

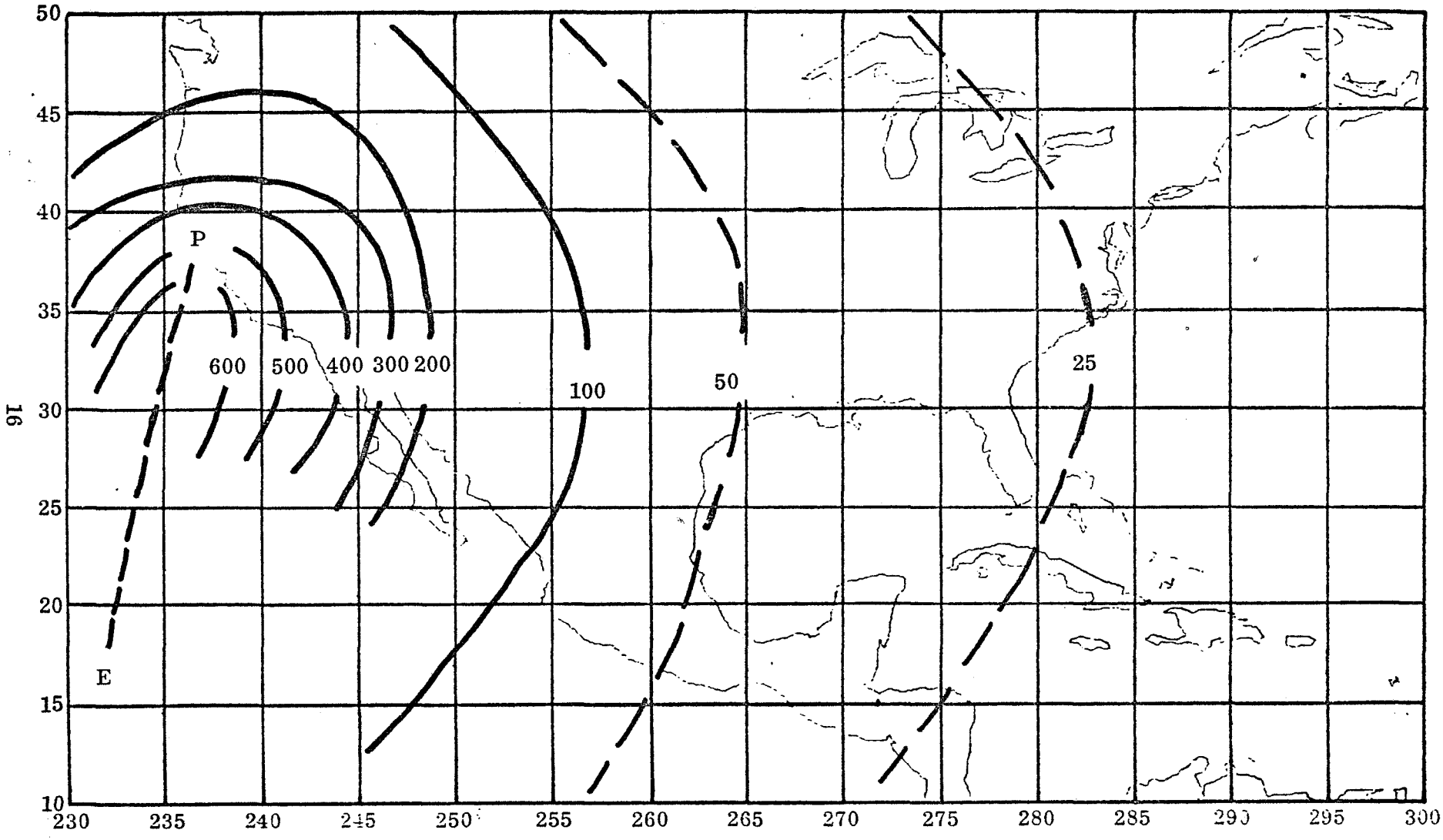

Fig. 7. Sensitivities of $\dot{\rho}$ in thousandths of a millimeter per second to φ in milligals. One satellite in a 700 km high orbit is tracked by a very high geostationary satellite. E denotes the position of the low satellite at the initial epoch, and P denotes its position at the epoch for which the partial derivatives are evaluated.

and descending passes.

2.15 Solutions Using Simulated Data.

The first question investigated was the size of blocks that could be resolved by two satellites close together in low orbits. An altitude of 700 km was chosen as representative, since orbits much lower than this are increasingly perturbed by air drag. Observation equations were generated from a set of 21 passes, with the two satellites separated by 200 km in the same orbit. Figure 8 shows the uncertainties of the recovered values of the density parameters in 92 $5^\circ \times 5^\circ$ blocks. The correlation coefficient between the recovered value of the density in a block and that of its neighbor to the east or west ranged from -0.70 to -0.90. This solution was judged to be marginally satisfactory, indicating that $5^\circ \times 5^\circ$ blocks can just barely be resolved from an altitude of 700 km.

A series of solutions was performed in which the two satellites were in orbits 300 km high. Several solutions showed that it is not always necessary to configure the two satellites so that one is always behind the other in the same orbit. Rather, it was found advantageous to introduce some variation in the relative configuration of the two satellites by using some passes in which the two satellites were roughly side by side in slightly different orbital planes, and by varying the separation between the two satellites. Figure 9 shows the uncertainties of the density parameters recovered with data from 18 passes at 300 km altitude. Typical correlations between the recovered values of the density in neighboring blocks are described by the correlation pattern below.

1.0	-0.60	0.20
0.40	-0.30	0.20
0.40	-0.30	0.15

In this pattern, positional displacement from the upper left hand corner indicates the relative position of the two blocks to which the given correlation coefficient applies.

In these adjustments, simulated observations of the positions of both satellites

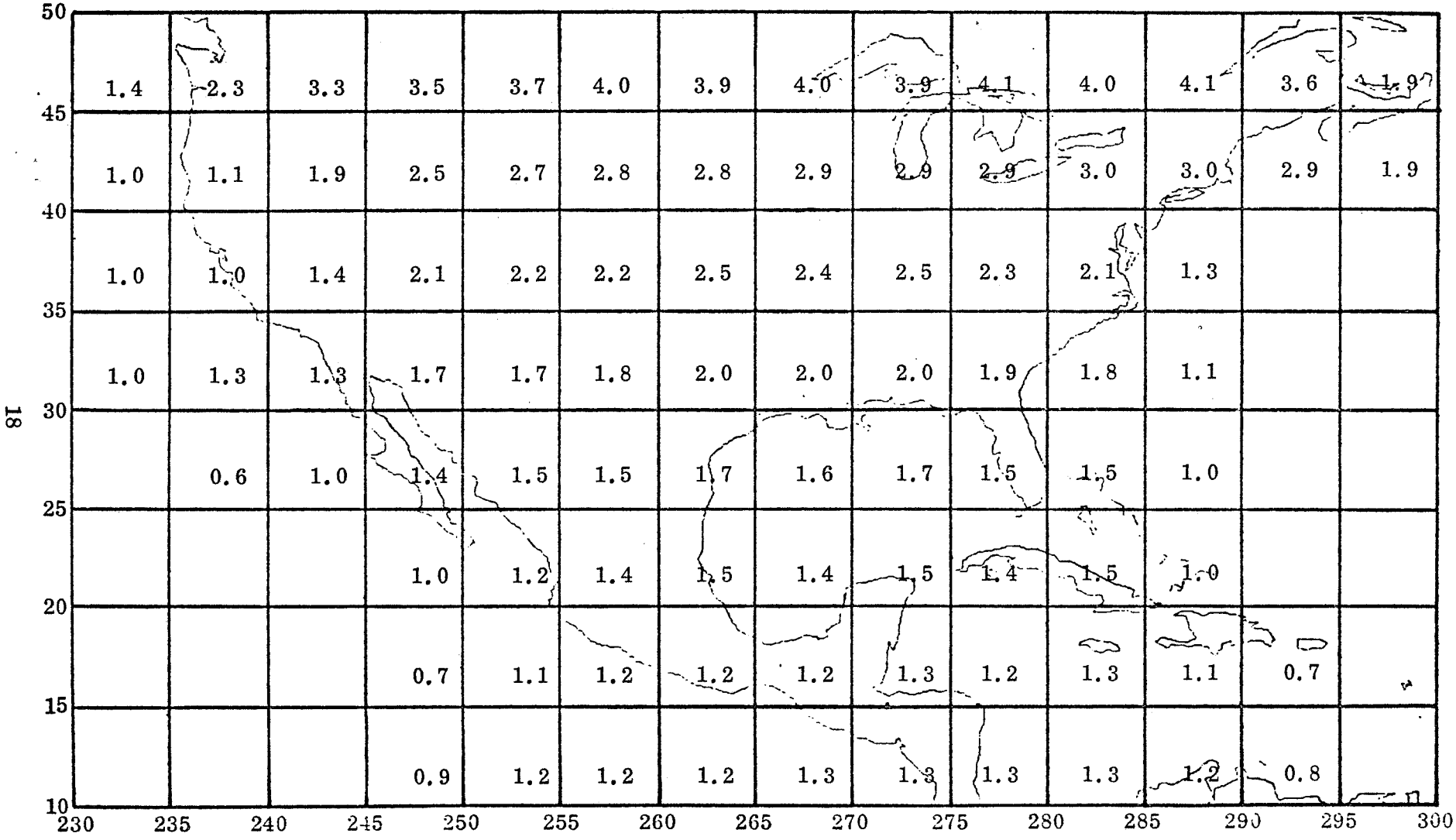

Fig. 8. 21 passes at 700 km. Uncertainties of the recovered values of the density parameter in $5^\circ \times 5^\circ$ blocks (mgals).

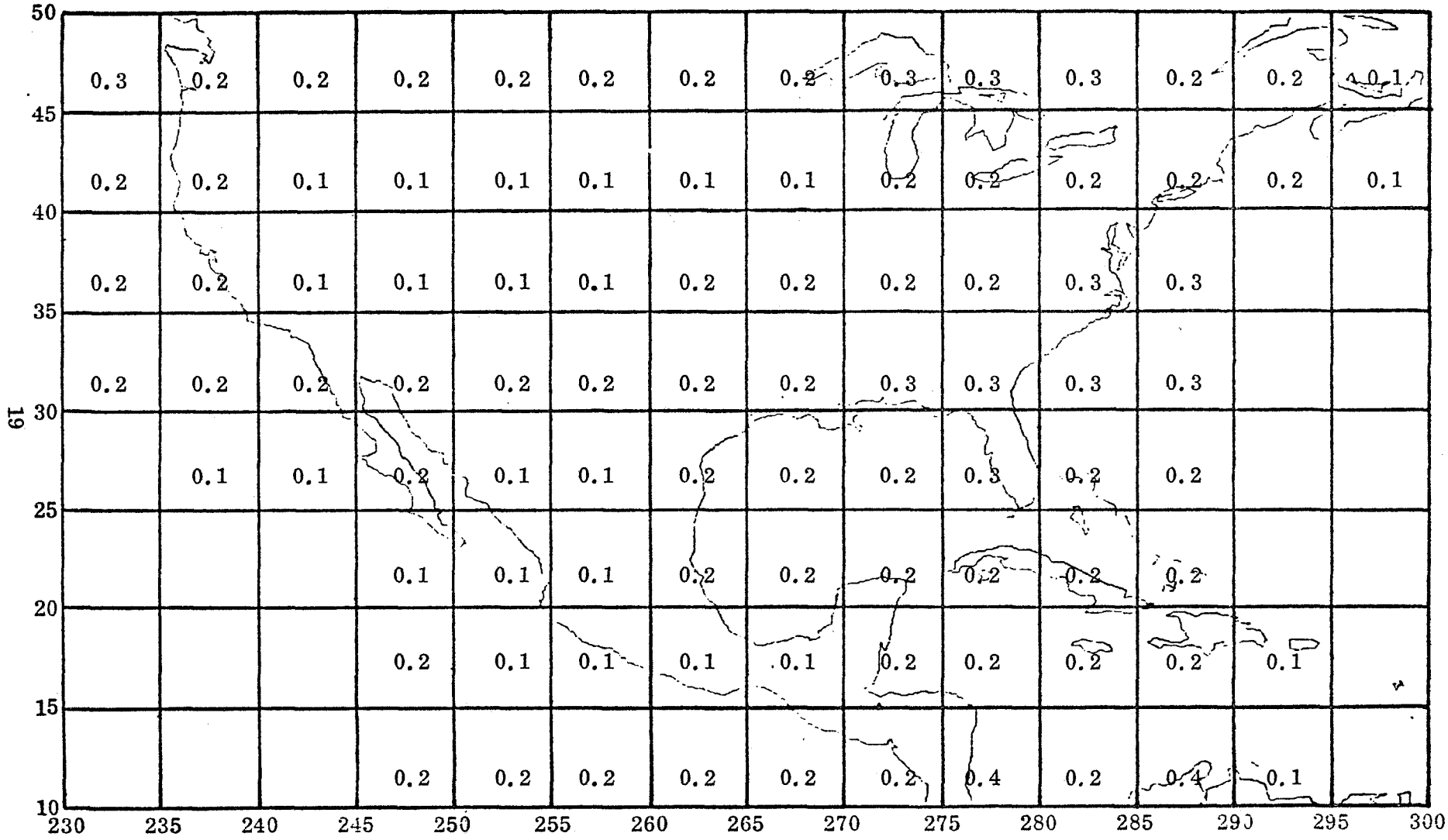

Fig. 9. 18 passes at 300 km. Uncertainties of the recovered values of the density parameter in $5^\circ \times 5^\circ$ blocks (mgals).

were used, as well as the simulated observations of the range rate between the two satellites. The position observations were assigned very low weights, and were included only to assign a geographic position to the gravimetric phenomenon being observed. Several adjustments showed that these position observations are necessary. However, it makes little difference to the solution for the gravity field parameters whether the accuracy with which the positions of the satellites are observed is 10, 100, or even 1000 meters in each coordinate. These experiments showed that some ground tracking of the two satellites is necessary, although there is absolutely no need for high accuracy tracking from the ground.

Another series of experiments used orbits 200 km high. This was judged to be about the lowest altitude at which a satellite might reasonably be kept in orbit for a reasonable lifetime, even with a drag compensation device. Satellite to satellite range rate observations were generated for 10 passes over a $10^\circ \times 10^\circ$ area, and solutions were made for the mean values of the density parameters in 25 $2^\circ \times 2^\circ$ blocks. Figure 10 shows the uncertainties in the recovered parameters when the satellites are separated by about 200 km in 200 km high orbits. Figure 11 shows the uncertainties when only one satellite is in a low orbit and the other is in a geostationary orbit high above the equator. A typical pattern of correlation coefficients for the case when both satellites are in low orbits is shown below.

1.0	-0.80	+0.45
-0.60	+0.40	-0.20
+0.35	-0.20	+0.10

When a single low satellite is tracked by a very high satellite, the correlation between pairs of blocks is slightly larger and falls off more slowly with distance between the two blocks. Typical correlation coefficients are shown for this case by the four block pattern below.

1.0	-0.80	+0.50	-0.35
-0.75	+0.60	-0.40	+0.25
+0.50	-0.40	+0.30	-0.15
-0.30	+0.25	-0.15	+0.10

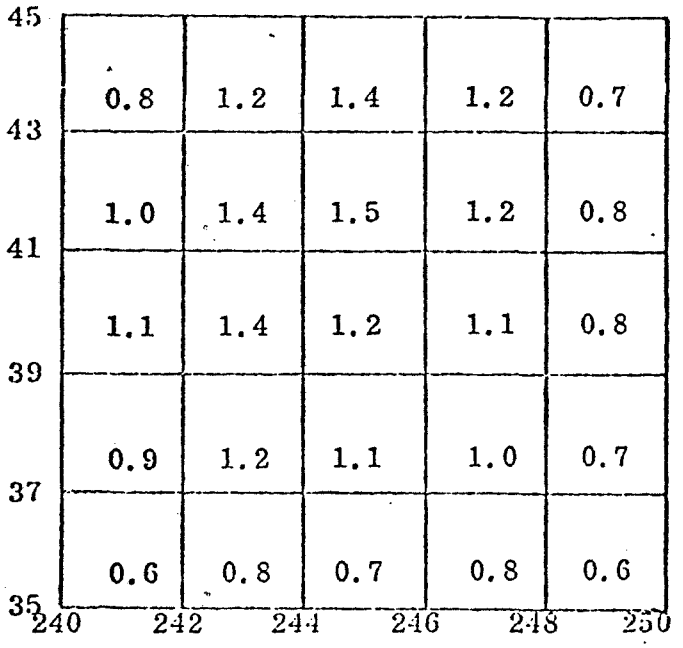

Fig. 10 Uncertainties of recovered values of the density parameters in $2^\circ \times 2^\circ$ blocks (mgals). Low-low Configuration.

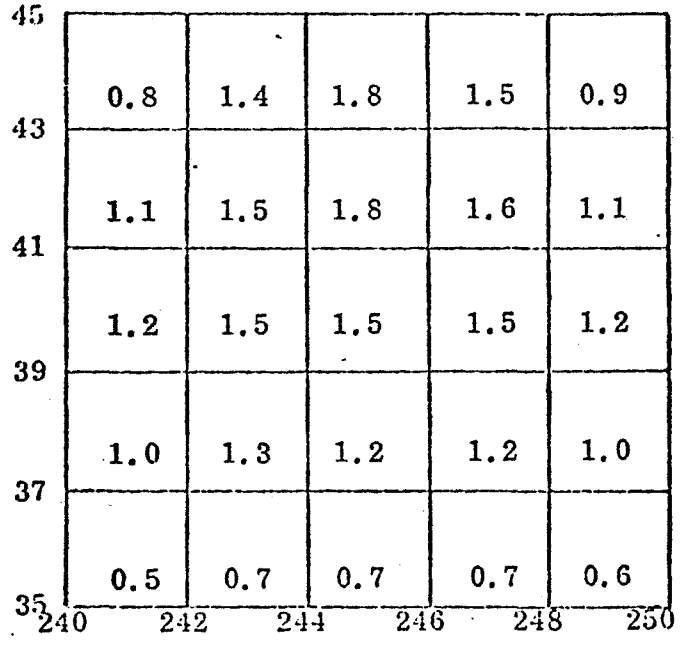

Fig. 11 Uncertainties of recovered values of the density parameters in $2^\circ \times 2^\circ$ blocks (mgals). High-low Configuration.

Both the uncertainties of the recovered parameters and the correlation coefficients indicate that better results are obtained with both satellites in low orbits. On the other hand, both solutions could be judged to be marginally acceptable, indicating that $2° \times 2°$ blocks can just barely be resolved from orbits 200 km high. To confirm this, several attempts were made to solve for the mean values of the density parameters in $1° \times 1°$ blocks. These adjustments were overcome with numerical error and produced completely unsatisfactory results. This remained true even when the satellite altitude was brought down to the unrealistic value of 100 km.

2.16 Conclusions.

If 200 km is accepted as the lowest altitude at which a satellite can be kept in orbit for a reasonable lifetime, then the gravity field can be resolved into $2° \times 2°$ blocks. A solution for blocks of this size on a global basis would be equivalent to determining the coefficients in the spherical harmonic representation of the geopotential through degree and order 90.

Larger blocks can be resolved from proportionally higher altitudes. An approximate relationship between block size and altitude is shown in Figure 12.

Although slightly better results are obtained with two low satellites than when a geostationary satellite tracks a single low satellite, many operational considerations argue strongly for the latter concept. Among these are the facts that only the low satellite would need to be equipped with a drag compensation device, and that the problem of data storage and later readout could be avoided. For these and other reasons, the concept of a constellation of geostationary satellites which track one or more minimum altitude satellites is recommended.

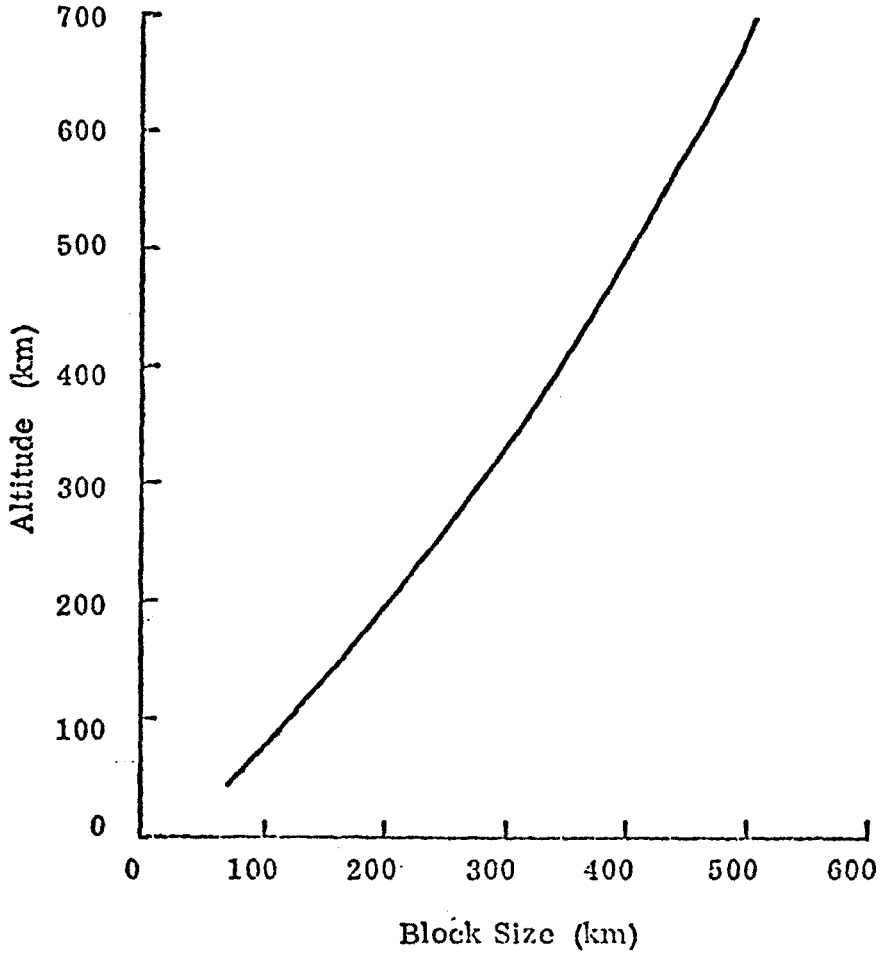

Fig. 12 Approximate Maximum Altitude From Which the Gravity Field Can Be Successfully Resolved, as a Function of Block Size.

2.17 References.

Gaposchkin, E.M. (1970). "The 1969 Smithsonian Standard Earth and Global Techtonics." Proceedings of the GEOS-2 Program Review Meeting 22-24 June 1970, (Vol. 1). Edited by Computer Sciences Corporation, 6565 . Arlington Boulevard, Falls Church, Virginia.

Kaula, William (editor). (1969). "Solid Earth and Ocean Physics." Report of a study at Williamstown, Massechusetts, to the National Aeronautics and Space Administration. Sponsored by NASA-Electronics Research Center, MIT-Measurement Systems Laboratory, Cambridge, Massachusetts. August.

Schwarz, Charles R. (1970). "Gravity Field Refinement by Satellite to Satellite Doppler Tracking." Report of the Department of Geodetic Science No. 147. The Ohio State University, Columbus.

Wolff, Milo (1969). "Direct Measurements of the Earth's Gravitational Potential Using a Satellite Pair." Journal of Geophysical Research, Vol. 74, p. 5295.

2.2 Investigations of Critical Configurations for Fundamental Range Networks.

A range network, formed by a set of ground stations and a set of targets is such that between the two sets of points only ranges are observed. As in most geodetic adjustments, the mathematical model for range observations is treated in a linearized form. The adjustment procedure applied to this model is the least squares method.

Range observations being invariant with respect to the coordinate system, they do not offer information about it; thus when an adjustment is performed in terms of coordinates a certain coordinate system has to be defined. Six constraints are necessary for definition of the coordinate system; three to define its position and three to define its orientation. Any coordinate system thus defined yields theoretically the same adjusted values of distances. In the theoretical part of this investigation, a coordinate system is chosen such that the first ground station is at its origin, the second one on its x axis and the third in its xy plane. For practical computations, that coordinate system may be the most advantageous which renders the trace of the variance-covariance matrix for the coordinates of all or certain selected points a minimum. The constraints defining the coordinate system in this manner are called "inner adjustment constraints". The idea of using inner adjustment constraints was first presented in [Meissl, 1962], and recently in [Rinner, 1966], Annex F and in [Meissl, 1969]. The problem of inner adjustment constraints is treated in great detail in [Blaha, 1971a]. Their application in connection with an actual adjustment appeared in [Mueller et. al., 1970].

When only six coordinate-system-defining constraints are used, the network is said to be fundamental. In this paper, only fundamental networks are considered. In certain cases when ground stations and/or targets are situated in special configurations, a unique adjustment in terms of coordinates may be impossible even if the number of observations is sufficient and the coordinate system is uniquely defined. Such critical configurations result in singular solutions and their description is the subject of this paper. They are separated into two groups. In the first group all ground stations are in a plane and in the second they are generally distributed. To a limited degree these problems were also treated in [Rinner, 1966], Annex A and in [Killian and Meissl, 1969]. Their detailed treatment is presented in [Blaha, 1971b], of which this paper is a summary.

2.21. Treatment of Range Observations with All Ground Stations in a Plane

The results of this section can be used for practical problems whenever the ground stations lie near a plane. Clearly, this happens when the ground network extends over a relatively small area.

The basic idea used in treating the networks where the ground stations are approximately in one plane is to stipulate that all ground stations are exactly in the plane and to find the critical loci of the points in the network which will result in a singular solution. Applications for practical cases (where the condition of coplanarity is only approximately fulfilled) follows from the fact that conditions leading to singularity in theory lead to near singularity in practice. Examples of the correspondence between such theoretical and practical configuration-conditions are the following:

(a) Targets on a straight line in theory correspond to satellite positions on a relatively short pass in practice.

(b) Ground stations lying on a second order (plane) curve in theory correspond in practice to ground stations in pro-

jection on the (best fitting) plane lying on or near a second order curve.

(c) A satellite group lying theoretically in a plane corresponds in practice to short satellite passes of approximately the same altitude. This situation can arise when the same satellite is observed on different passes.

The main result of this investigation is the detection of singularity for the theoretical cases and the establishment of rules to avoid it.

In order to present the results of these investigations, certain notations are introduced: The ground stations are denoted by numbers and letters in the sequence 1, 2, 3, 4, ... i ..., k, s′, s″, ..., while the satellite groups observed by these stations are denoted as j_4, ... j_i ..., j_k, $j_{s'}$, $j_{s''}$ ..., respectively. A satellite group consists of those satellite points (targets) which are observed by a given quadrant (quad) of stations. The convention used for the subscript of a certain satellite group is such that the index indicates the number or letter of that station in the quad observing this satellite group which has not observed any other satellite group and/or which is listed as the last station in the quad. For example, the quad consisting of stations 1, 2, 3, and 4 observes the satellite group j_4. The division of a network into quads is convenient from the practical point of view. Considering more than four co-observing stations does not affect the derivations made with the above concept.

The discussion is divided into two basic parts, according to whether the number of ground stations observing all the satellite points is three or more, or less than three. When the number of stations observing all the targets is less than three the principle of "station replacements" is introduced which leads directly to the concept known in practice as "leapfrogging". Both concepts, the first, dealing with at least three stations observing all the targets, and the second, dealing with replacing of stations,lead to similar conclusions. The

most important conclusion is that except for certain critical configurations of points (stations or targets or both) an adjustment of range networks gives non-singular results, in spite of the fact that all stations are in one plane. The network which can be non-singular with the smallest number of ground stations possible is said to constitute a fundamental unit. When at least three stations observe all the targets a fundamental unit consists of six stations. When the principle of station replacement is utilized a fundamental unit is also six stations, except for one specific observing pattern when the number of required stations is seven.

When three stations denoted as 1, 2, 3 are observing all the targets, the necessary and sufficient conditions for a network to be non-singular are easy to specify. One of the configurations which makes an adjustment singular is the case when all the targets in one satellite group needed for the determination of a fundamental unit are in a straight line. This is only a special case of a general pattern when all satellite points within a group (e.g., j_1) are in the plane containing the corresponding ground station (i). This case, called singularity A) is illustrated in Figure 13. In a more general sense, singularity A) is said to occur when all targets observed by a certain station - and such targets may be contained in more than one satellite group - are in the plane with this station. When exactly three stations (1, 2, 3) observe all targets, the targets observed by any particular station besides 1, 2, 3, are all contained in one satellite group. Under the assumption that singularity A) does not exist the necessary and sufficient conditions for a network to be non-singular are such that at least three stations in addition to those three (1, 2, 3) observing all the targets must observe targets which are not all in one (general) plane (off-plane targets), and that these three stations must not lie on one second order curve with stations 1, 2, 3. If these conditions are not fulfilled it is said that singularity C) has occurred; such configuration of points is illustrated in Figure 15. A special case of singularity C) is singularity B) when all the ground stations are on one second order

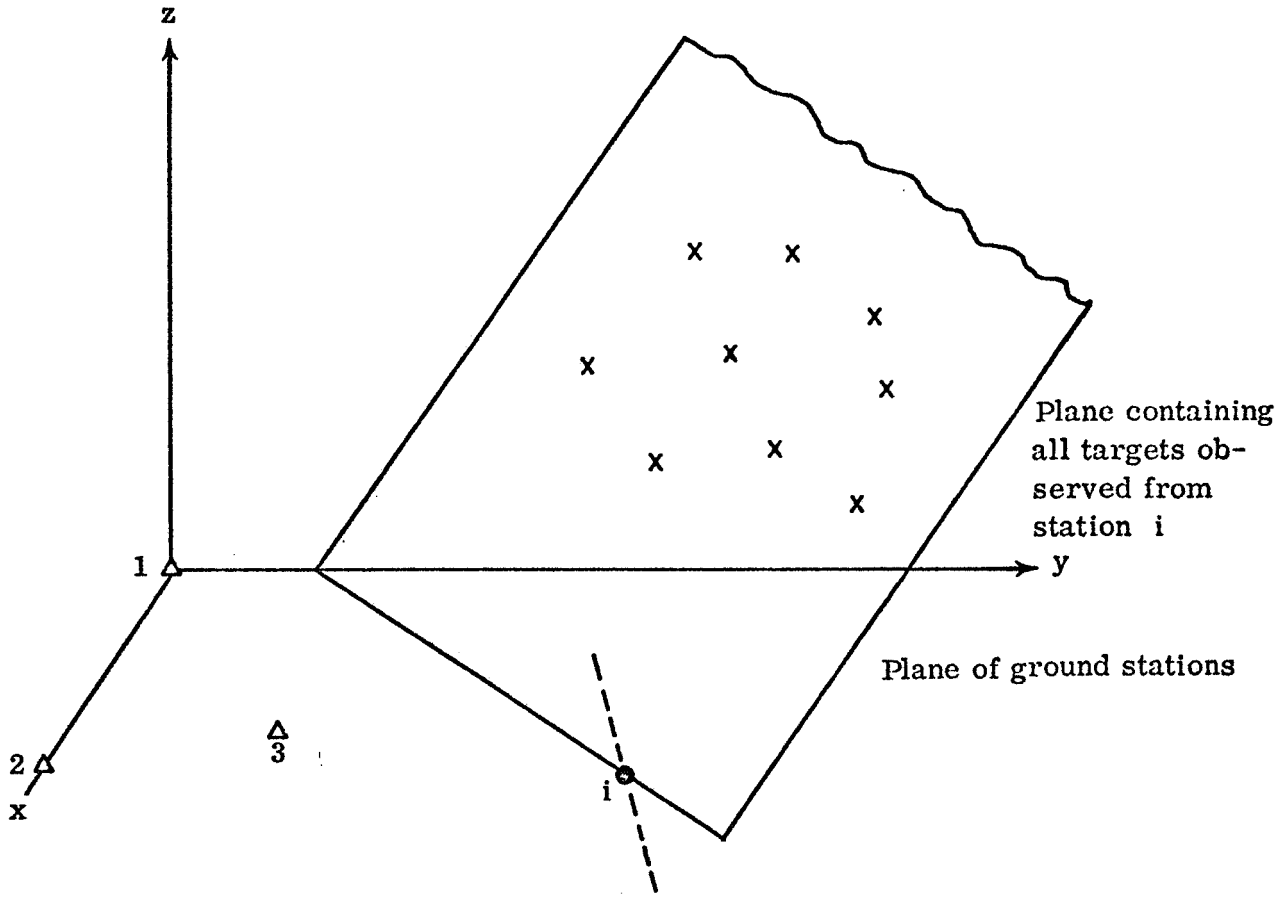

Figure 13

ILLUSTRATION OF SINGULARITY A): Station i is in the plane of its observed targets.

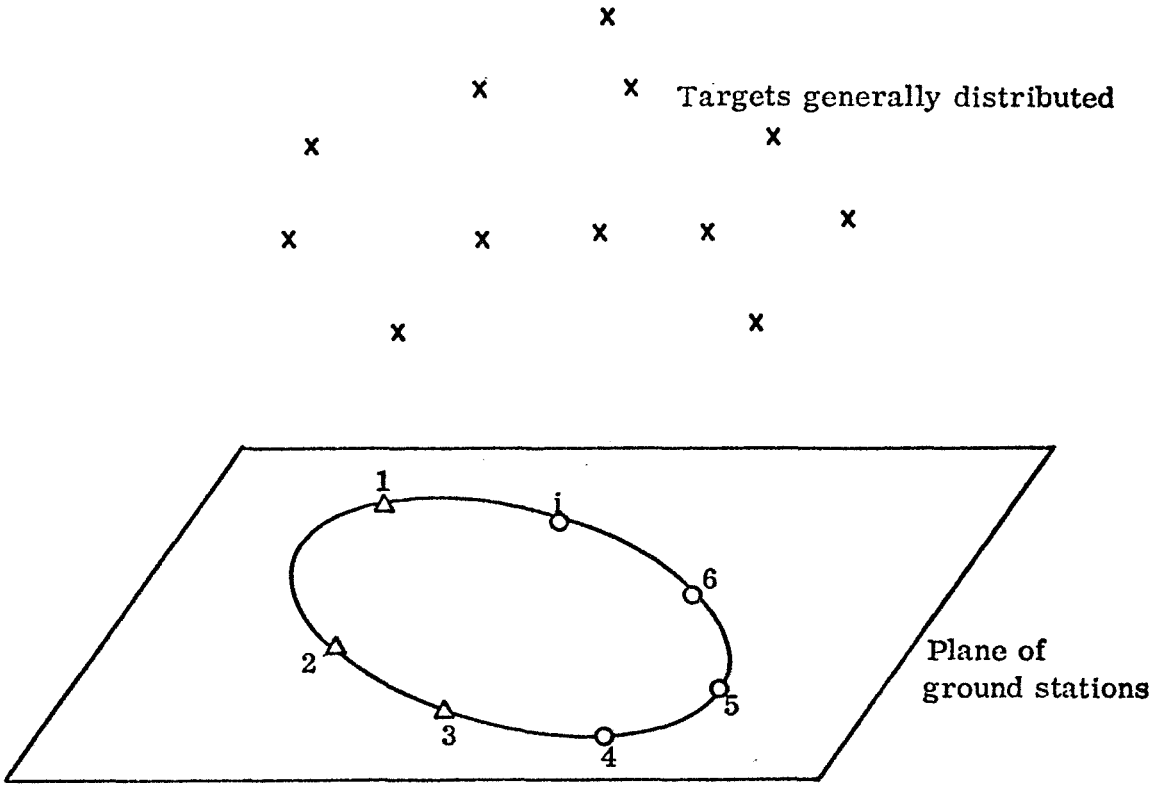

Figure 14

ILLUSTRATION OF SINGULARITY B): Stations 1, 2, 3 observe all targets; all stations are on a second order curve.

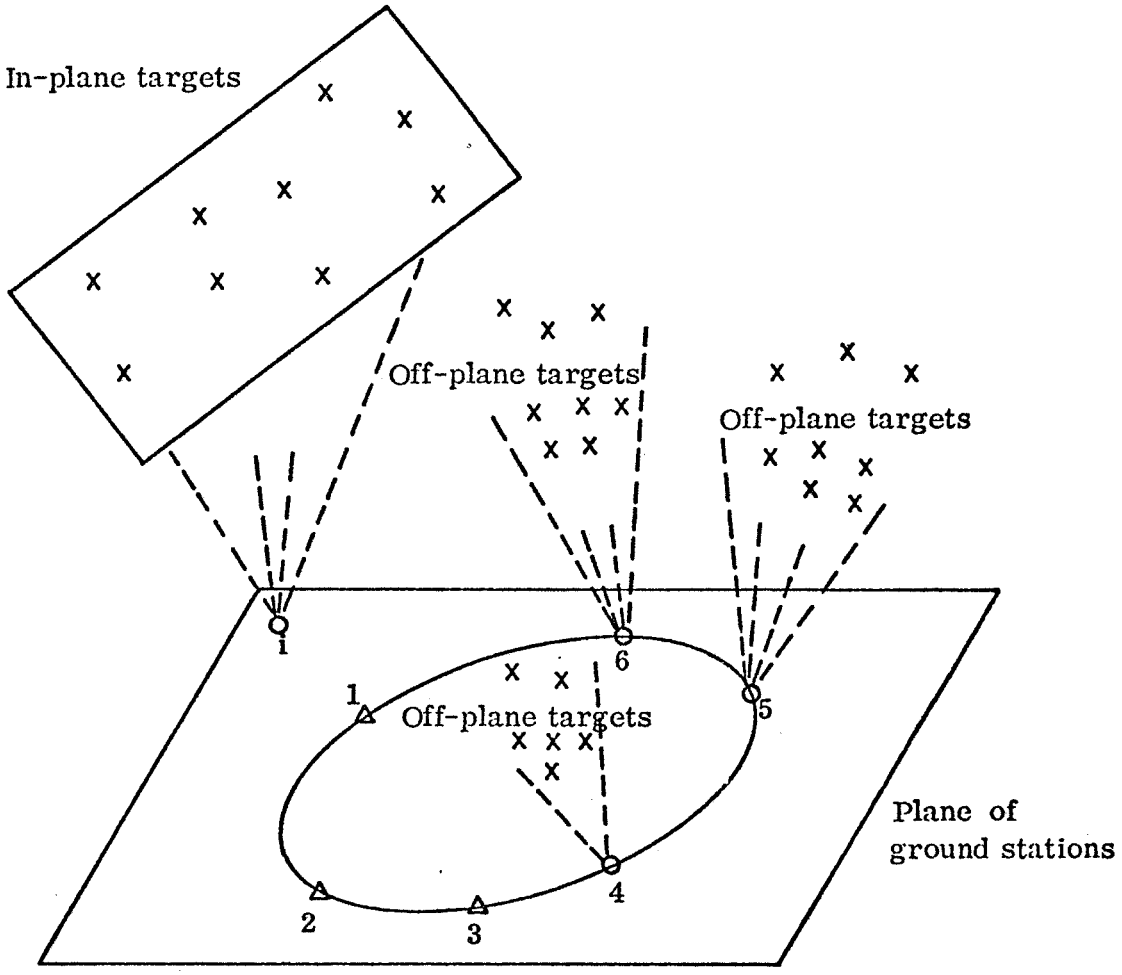

Figure 15

ILLUSTRATION OF SINGULARITY C): Stations 1, 2, 3 observe all targets; all stations observing off-plane targets are on a second order curve with stations 1, 2, 3.

curve (Figure 14). From the above conditions it is seen that a fundamental unit consists of six ground stations. If such a fundamental unit exists, it is always possible to expand a network by adding further stations and satellite groups, the necessary and sufficient conditions being that no target should lie in the plane of the ground stations and that no station should lie in a plane with all its observed targets.

If all ground stations are co-observing, then singularity in a network could occur only if all the stations are on one second order curve, or if all the targets (in this case all the satellite groups coincide) are in one plane. These two cases are illustrated in Figures 16 and 17, respectively. Otherwise, the solution is non-singular. Numerical results indicated that when all the stations observed simultaneously the solution was strengthened very significantly.

When dealing with the concept of station replacement, it is concluded that one replacement (leapfrogging) can be sufficient to build a fundamental unit, from which further expansion is possible under certain conditions. Therefore, a great deal of time was devoted analyzing the problem of one replacement where the fundamental unit is assumed to comprise of stations $1, 2, 3, 4$, and the satellite group j_4 to contain off-plane targets. After two quads (formed by stations $1, 2, 3, 4$, and stations $1, 2, 3, k$) have completed their observations, the first replacement will take place. It consists of station k replacing station 3 for the next observations. The satellite group $j_{s'}$ is then observed by the quad of stations $1, 2, k, s'$, etc. At this point, the discussion is divided into two cases: in the first case the satellite group j_k contains off-plane targets; in the second case, which is rather special and mainly of theoretical interest, the targets in j_k are in one plane. It is true for both cases that a network is singular if the targets in any of the satellite groups (including j_k in the second case) are in a straight line. This conclusion is similar to what was mentioned for three stations observing all the targets. It is again assumed that no satellite group lies in a plane passing through the corresponding station. Thus, singularity A) cannot exist.

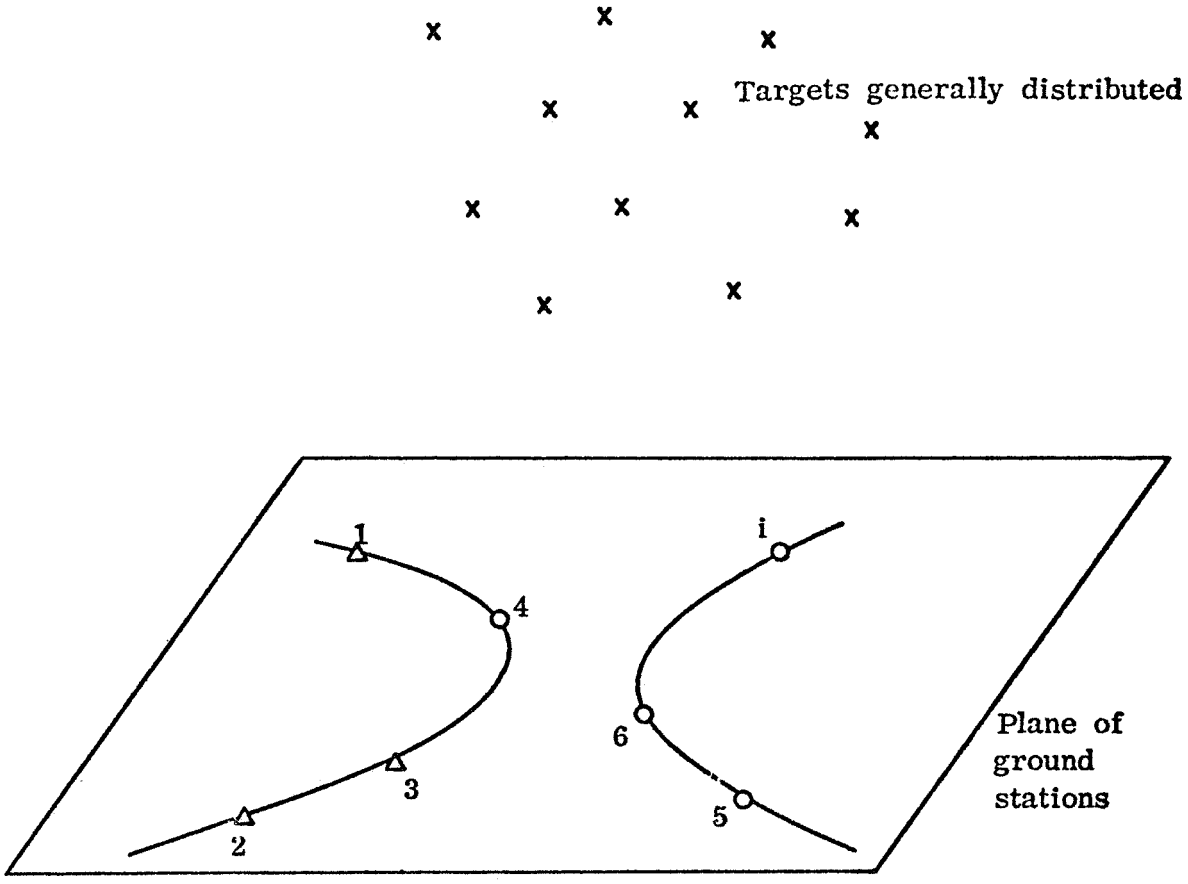

Figure 16

ILLUSTRATION OF SINGULARITY C): All stations observe all targets; all stations are on a second order curve.

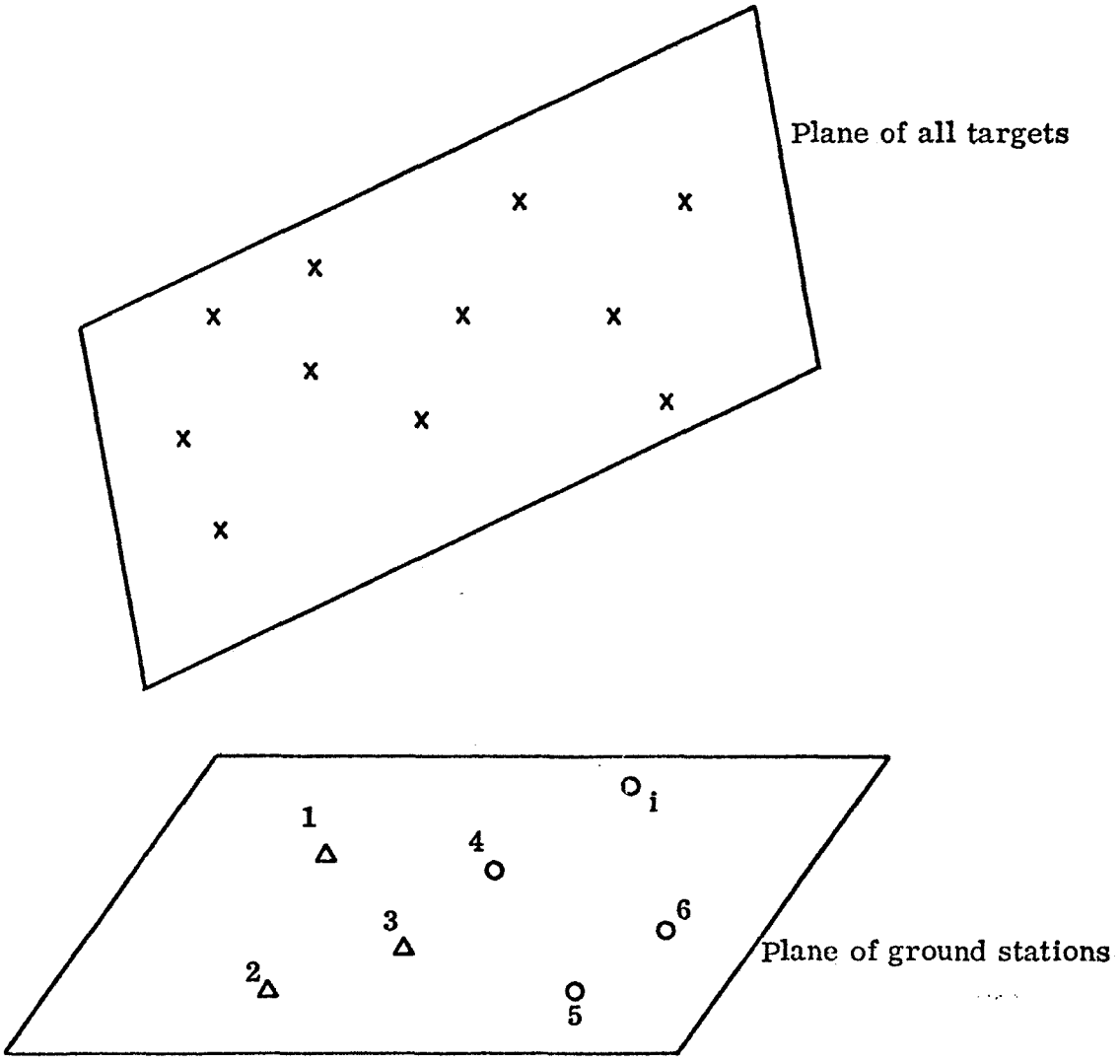

Figure 17

ILLUSTRATION OF SINGULARITY C): All stations observe all targets; all targets are in a plane.

With the above assumption, the necessary and sufficient conditions for a non-singular solution in the first case (j_k containing off-plane satellites) are similar to those given for three stations observing all the targets. Namely, the network is non-singular if there is at least one more satellite group (in addition to j_4 and j_k) containing off-plane targets and if the corresponding station does not lie on a second order curve with stations 1, 2, 3, 4, and k. In other words, at least three stations not lying on a second order curve with stations 1, 2, 3 must observe off-plane targets. Therefore, a fundamental unit in this case consists also of six ground stations.

The second case, rather artificial, deals with such configurations when the satellite group j_k is composed of targets lying all in one plane (assumed not to pass through station k). The necessary conditions for a non-singular network stipulate that there must be at least two additional satellite groups (besides j_4) which contain off-plane targets. Consequently, a fundamental unit in this case includes seven ground stations (i. e., two stations in addition to stations 1, 2, 3, 4, and k).

If the first replacement is successfully carried out, then the resulting fundamental unit can be expanded to become a larger, non-singular network. When new stations and satellite groups are added to it, the necessary and sufficient conditions for the new network to be non-singular are the same as those for similar enlargement when three stations observed all the targets; namely, no target should be in the plane of the ground stations and no station should be in a plane with all its observed targets.

The main results of this section are summarized in Table 1.

Since the number of ground stations is always relatively small compared to the number of targets, the most important conclusion for all ground stations lying in a plane is that the ground stations should not be distributed on or near a second order curve.

Table 1.

Necessary and Sufficient Conditions to Avoid Singular Solutions

When All Ground Stations Are in a Plane

Type of Singularity	Arrangement of Observations		Necessary Conditions to Prevent Singularity	Sufficient Conditions to Prevent Singularity	Note
Singularity A) (or closely related singularity)	Any		No station should be in a plane with all its observed targets (distributed over one or more satellite groups)	No station should be in a plane with the corresponding satellite group	This singularity is assumed non-existent in analysis of singularity C)
Singularity C) (global type of singularity)	Stations 1, 2, 3 observe all targets		Three stations in addition to 1, 2, 3 not lying on a second order curve with them should observe off-plane targets	The same as the necessary conditions	Special case of singularity C) is singularity B); it occurs when all stations are on a second order curve
	Station k replaces station 3 (satellite group j_4 contains off-plane targets)	Group j_k contains off-plane targets	One station in addition to 4 and k not lying on a second order curve with 1, 2, 3, 4, k should observe off-plane targets	The same as the necessary conditions	
		Group j_k contains in-plane targets	Two stations in addition to 4 should observe off-plane targets. Always: Avoid all stations lying on a second order curve	More complex requirements (according to stations which observe off-plane targets)	
	All stations observe all targets (all stations co-observe)		Avoid all targets lying in a plane (any plane) and all stations lying on a second order curve	The same as the necessary conditions	

2.22 Treatment of Range Observations with Ground Stations Generally Distributed

In this section the ground stations in fundamental range networks are considered to be generally distributed in space. This discussion covers range observations made over a large territory, when ground stations are on the physical surface of the earth, departing significantly from a plane. Since the ground stations in this instance are all approximately on a sphere, their distribution in space is not completely general. However, whenever they depart from a plane, the nature of the problem is the same regardless of further specifications.

The observations are again divided into quads with similar notations as those used previously. Whether four or more ground stations observe simultaneously has again no effect on the derivations. Most of the investigations for general distribution of ground stations have been carried out for at least three stations observing all the targets.

Perhaps the most important theoretical result in this section is that whenever all the points (ground stations and targets) of a network lie on one second order surface the network is necessarily singular. An illustration of such configuration appears in Figure 19.

Some special cases of singular solutions arise when all the targets observed by a certain station (they can be in one or more satellite groups) are in a plane which contains this station (mostly called singularity A)), or when all the targets of a network are in a plane on a second order curve (called "reversed singularity B)"). When all its points lie on a second degree surface, the network is singular even if all the ground stations co-observe; this is the only case of a singular problem when all the stations co-observe, except for the special cases when all the targets of a network are in a plane containing one ground station, or when they are all on a second order (plane) curve. Naturally, when all the points are on one second order surface, the network is singular no matter how the observations are arranged ("leapfrogging", etc.).

When only a limited number of stations co-observe, the situation is somewhat more complicated. In practice, four stations forming quads may co-observe a set of targets. With three stations observing all the targets, it was found that an adjustment of range observations is singular if for each quad the stations and the corresponding targets lie on a specific second order critical surface. All these critical surfaces intersect in one second order (plane) curve containing the above three stations. This geometric property is illustrated in Figure 18. If the special singular cases due to singularity A) or "reverse singularity B)" do not exist, the network has a non-singular solution if there is at least one (satellite) point located outside the corresponding critical surface.

When utilizing the concept of station replacement, it was found that besides the above two special cases singular solutions would again be associated with specific second order surfaces. In this case, sufficient conditions for non-singular networks stipulate that after an expansion of a non-singular network the new network is still non-singular if the targets of any "new" satellite group do not lie in a plane with the "old" three stations and that the fourth, "new" station does not lie in one plane with these targets.

The main results of this section are summarized in Table 2.

It can be concluded that with singularity A) and reverse singularity B) non-existent, a solution will be singular if certain (or all) stations together with certain (or all) satellite points lie on specific second order surface(s). However, such cases are not likely to happen in practice for the following reasons:

(a) Distribution of ground stations alone does not induce any type of singularity. Since the number of ground stations is always limited, their distribution presented a cause for concern in the limited area (plane) case; it is irrelevant in the general distribution case.

(b) If a network is singular, it is caused by all the satellite points lying on certain second order surfaces (together with some ground stations). This could seldom happen in

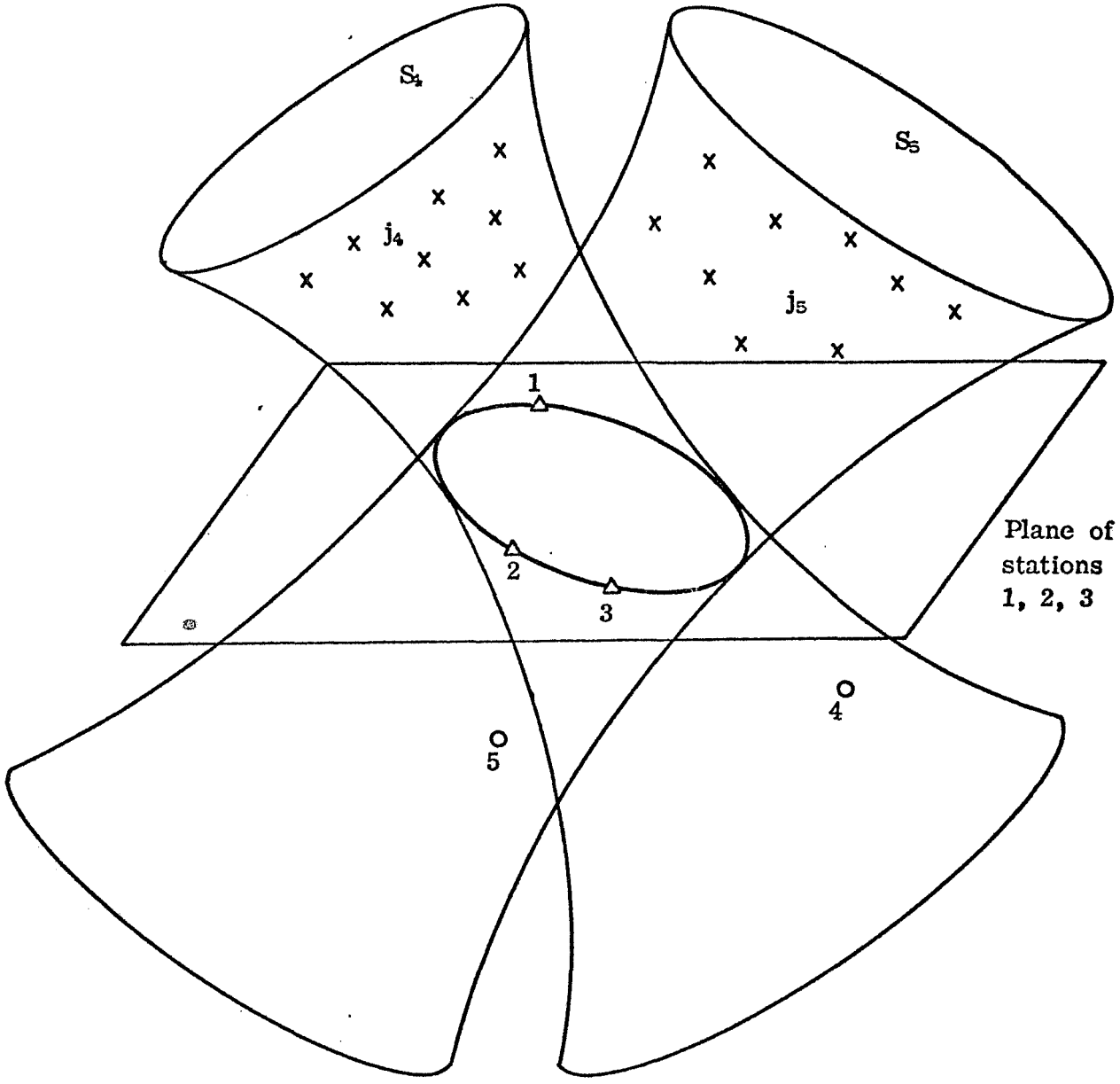

Figure 18

ILLUSTRATION OF CRITICAL SURFACES: Stations 1, 2, 3 observe all targets; stations 4 and 5 together with their satellite groups j_4 and j_5 are on the second order surfaces S_4 and S_5, respectively; stations 1, 2, 3 are on the second order intersection curve of surfaces S_4 and S_5.

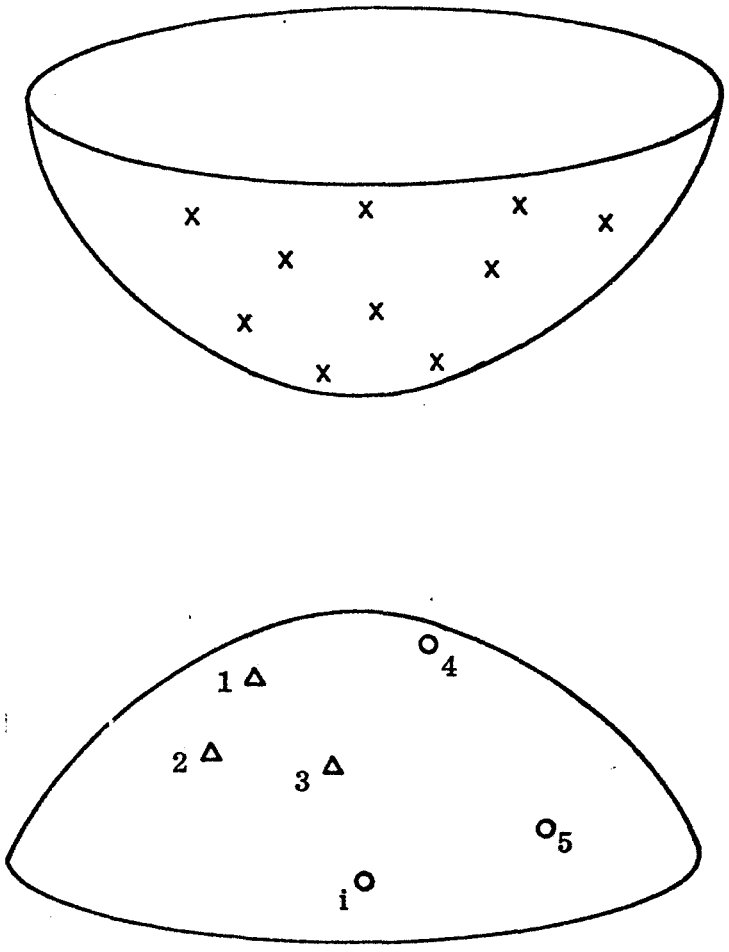

Figure 19

ILLUSTRATION OF CRITICAL SURFACES: All stations observe all targets; all stations and all targets are on a second order surface.

Table 2.

Necessary and Sufficient Conditions to Avoid Singular Solutions

When Ground Stations Are Generally Distributed

Type of Singularity	Arrangement of Observations	Necessary Conditions to Prevent Singularity	Sufficient Conditions to Prevent Singularity	Note
Singularity A) (or closely related singularity)	Any	No station should be in a plane with all its observed targets (distributed over one or more satellite groups)	No station should be in a plane with the corresponding satellite group	This singularity is assumed non-existent in analysis of global singularity
Reversed Singularity B)	Any	Targets should not be all in a plane on a second order curve	The same as the necessary conditions	This singularity is assumed non-existent in analysis of global singularity
Global Singularity	Stations 1, 2, 3 Observe all targets	Avoid all satellite groups (one group per quad) containing targets lying all on the corresponding second order critical surfaces (one surface per quad). Always: Avoid all points lying on a second order surface	The same as the necessary conditions	All the critical surfaces can be computed explicitly. They all intersect in the plane of stations 1, 2, 3 on a second order curve containing the three stations. If four points outside this plane are common to some critical surfaces then these surfaces coincide
	Station replacement (e.g., leapfrogging)	Always: Avoid all points lying on a second order surface	Avoid certain second order surfaces not expressed explicitly	
	All stations observe all targets (all stations coobserve)	Avoid all points lying on a second order surface	The same as the necessary conditions	

practice as the number of targets may be very large; thus the probability of all the targets lying on specific second order surfaces is very small.

Results of the range investigations for ground stations in general configuration can be certainly useful when only a small number of targets is observed because then it could happen that they all lie near one or more specific second order surfaces. However, for the reasons cited above, these results are mainly of theoretical interest.

2.23 References.

Blaha, Georges. (1971a). "Inner Adjustment Constraints with Emphasis on Range Observations." Reports of the Department of Geodetic Science, No. 148, The Ohio State University, Columbus.

Blaha, Georges. (1971b). "Investigations of Critical Configurations for Fundamental Range Networks." Reports of the Department of Geodetic Science, No. 150, In press, The Ohio State University, Columbus.

Killian, Karl and Peter Meissl. (1969). "Einige Grundaufgaben der räumlichen Trilateration und ihre gefährlichen Örter." In Karl Rinner, Karl Killian, Peter Meissl, "Beiträge zur Theorie der geodätischen Netze im Raum." Deutsche Geodätische Kommission, Reihe A, No. 61.

Meissl, Peter. (1962). "Die innere Genauigkeit eines Punkthaufens." Österreichische Zeitschrift f. Vermessungswesen, Vol. 50, No. 5,6.

Meissl, Peter. (1969). "Zusammenfassung und Ausbau der inneren Fehlertheorie eines Punkthaufens." In Karl Rinner, Karl Killian, Peter Meissl, "Beiträge zur Theorie der geodätischen Netze im Raum." Deutsche Geodätische Kommission, Reihe A, No. 61.

Mueller, Ivan I., J.P. Reilly, Charles R. Schwarz, and Georges Blaha. (1970). "Secor Observations in the Pacific." Reports of the Department of Geodetic Science, No. 140, The Ohio State University, Columbus.

Rinner, Karl. (1966). Systematic Investigations of Geodetic Networks in Space. U.S. Army Research and Development Group (Europe), May.

2.3 Separating the Secular Motion of the Pole from Continental Drift.

2.31 Introduction.

Although paleomagnetic and other evidence argue strongly for the view that the continents have drifted apart from each other during geologic times, there has not yet been any geodetic determination of whether continental drift is occurring at the present time. Since it seems likely that the drifting motions of the continents are continuous rather than catastrophic in nature, detection of the present rates of continental drift will be a major goal of geodesy in the future. The accuracies of the station positions presently obtained from geodetic techniques are in the order of a few meters. However, it is probable that future observations will be sufficiently precise to detect motions of the continents relative to the pole and/or to each other, especially if highly precise geodetic networks are established and then re-observed after a period of several years or decades.

The purpose of this study was to predict the magnitude and direction of the motion to be expected at various geodetic and astronomical observatories, so that a judgment might be made of the time base necessary to detect continental drift.

There are several kinds of observations to be considered. First, the Very Long Baseline Interferometry (VLBI), which will define a few highly precise baselines whose length and orientation will be determined with precisions as high as one part in one hundred million. The second group of observations to be considered is the optical and laser observations of geodetic satellites and/or of the moon analyzed in the geometric (simultaneous) mode. These and the VLBI observations are ideal to determine the relative motions of the continents. For a complete description of these relative motions, the network should include at least three stations on each tectonic block. Optical and laser observations analyzed in the dynamic mode constitute a third group especially useful to detect motions in the absolute sense, i.e., relative to the Conventional International Origin (CIO). Similar purpose is served by the fourth group, the astronomic observations of observatories associated with the IPMS and the BIH which observe astronomic latitude and/or longitude. In order to separate continental drift from secular polar motion, both relative and absolute observations are needed.

2.32 Assumptions.

The basic assumption used in this study was the geometrical model of continental drift hypothesized by Le Pichon [1968]. According to this model, the surface of the earth consists of six large rigid plates in motion relative to each other. The only modifications of the rigid blocks occur along some or all of their boundaries. These boundaries are the crests of the mid-ocean ridges, and their associated transform faults, and the active trenches and regions of active folding or thrusting. The relative displacement of any block with respect to another is represented as a rotation on the spherical surface of the earth. That is, the spreading zones all lie along arcs of great circles, while the direction of motion and the transform faults lie along small circles perpendicular to the spreading zones. The spreading occurs around some pole of rotation which is associated with the spreading zone. Le Pichon used five principal spreading zones (and associated poles) and showed that the observed spreading rates and azimuths of the transform faults fit this model reasonably well. These spreading zones were then assumed to have known rates of opening (Table 3) and the rates of spreading or compression were then computed for the other boundaries of the six rigid blocks.

The Le Pichon model is expressed in terms of the relative movements of the six rigid blocks. However, it fails to predict the absolute motion of a point with respect to the solid body of the earth or with respect to the CIO. In order to determine how each block moves with respect to a coordinate system fixed in the solid earth, it is necessary to assume that one of the blocks remains fixed. For this purpose we chose the Antarctic block. There is no compelling reason for chosing the Antarctic block, since at present there seems to be no way of determining absolute motion. However, the fixing of Antarctica does fit the concept of Antarctica as the remnant of a protocontinent in the southern hemisphere from which South America, Africa, India, and Australia drifted northward. If the Antarctic block is not fixed with respect to the solid earth, then, in the concept of this study, the periodic mean pole of rotation is carried away from the CIO, thus an apparent secular motion of the pole is evidenced. Conversely, any observed secular motion of the pole can be eliminated in the concept of assigning this motion to the Antarctic block.

The latitude, longitude, and spreading rates associated with the centers of rotation given by Le Pichon may be considered as the polar coordinates of an angular velocity vector which characterizes the spreading motion. Thus,

if X is the position vector of a point on the North Atlantic rise and Ω_E is the angular velocity vector associated with the Arctic Ocean center of rotation (the subscript refers to the ordering in Table 3), then $\Omega_E \times X$ is the linear velocity vector giving the relative velocity between the American and Eurasian blocks at that point. Similarly, the expression $\Omega_A \times X$ will give the velocity, relative to Antarctica, of a point on the Pacific side of the South Pacific spreading zone. Since the Antarctic block is assumed to be fixed, this is also the absolute motion (relative to the solid earth). Since this expression is valid for all points along the spreading zone, it must be valid for the whole Pacific block. Thus, Ω_A is the angular velocity vector characterizing the rotational movement of the Pacific block. Since the angular velocities add vectorially, the angular velocities for the other blocks can also be worked out in this manner. The angular velocity vectors for the six rigid blocks, expressed in polar coordinates, are given in Table 4.

From these block motions, the relative motion along all block boundaries may be computed by taking the difference between the vectors associated with the respective blocks. By this method, Le Pichon computed his Table 4 [Le Pichon, 1968, p. 3676, and Le Pichon, 1970].

2.33 Predicted Motions.

With the model described in the previous section, it is possible to predict either the absolute motion of a single station or the relative motion of a pair of stations. Let station i be located on block k and let Ω_k be the components of the angular velocity vector associated with block k, resolved in Cartesian terrestrial coordinates. The components of the angular velocity vector, resolved in local coordinates at the station, can be obtained by a series of orthogonal matrix transformations [Arur and Mueller, 1971]. Thus,

$$R_2(\varphi_i)\, R_3(\lambda_i)\, \Omega_k = \begin{pmatrix} -\dot{A}_i \\ -\dot{\varphi}_i \\ \cos\varphi_i\, \dot{\lambda}_i \end{pmatrix}$$

where φ_i and λ_i denote the latitude and longitude at station i, and $\dot{A}_i$ denotes the variation in azimuth at the station. The rates of change of latitude and longitude, $\dot{\varphi}_i$ and $\dot{\lambda}_i$, may be taken directly from this equation.

Table 3

Centers of Rotation for the Five Principal Spreading Zones
(From Le Pichon [1968])

Pole	Latitude (deg)	Longitude (deg)	Angular Rate (10^{-7} deg/yr)
A. South Pacific (Antarctica-Pacific)	70 S	118 E	10.8
B. Atlantic (America-Africa)	58 N	37 W	3.7
C. North Pacific (America-Pacific)	53 N	47 W	6.0
D. Indian Ocean (Africa-India)	26 N	21 E	4.0
E. Artic Ocean (America-Eurasia)	78 N	102 E	2.8

Table 4

Angular Velocities of the Six Rigid Blocks
(Relative to Antarctica)

Block	Equation	Latitude (deg)	Longitude (deg)	Angular Rate (10^{-7} deg/yr)
1. Antarctica	$\Omega_1 = 0$	-	-	0.0
2. Pacific	$\Omega_2 = \Omega_A$	70 S	118 E	10.8
3. America	$\Omega_3 = \Omega_A + \Omega_C$	79.9 S	40.4 E	5.4
4. Eurasia	$\Omega_4 = \Omega_A + \Omega_C + \Omega_E$	62.9 S	70.0 E	2.9
5. Africa	$\Omega_5 = \Omega_A + \Omega_C + \Omega_B$	43.2 S	13.7 W	3.2
6. India	$\Omega_6 = \Omega_A + \Omega_C + \Omega_B + \Omega_D$	4.6 S	7.4 E	5.7

The linear velocity at any station is given by $V = \Omega \times X$. Let ΔV be the relative velocity vector between two stations, and let ΔX be their relative position vector. Further, let α, β, and D be the polar coordinates of the point whose Cartesian coordinates are the components of ΔX, i.e.,

$$\alpha = \tan^{-1}(\Delta y/\Delta x)$$

$$\beta = \sin^{-1}(\Delta z/D)$$

$$D = |\Delta X| = (\Delta x^2 + \Delta y^2 + \Delta z^2)^{\frac{1}{2}} .$$

Then α is the longitude direction component of the line between the two stations, β is the latitude direction component, and D is the length of the line. The rates of change of these components may be obtained from the equation

$$R_2(90^\circ - \beta)\, R_3(\alpha)\, \Delta V = \begin{pmatrix} -D\dot{\beta} \\ D\cos\beta\dot{\alpha} \\ \dot{D} \end{pmatrix} .$$

Thus $\dot{D}$ gives the predicted change in the length of a baseline between two stations on different blocks, and $\dot{\theta} = (\dot{\beta}^2 + \cos^2\beta\dot{\alpha}^2)^{\frac{1}{2}}$ gives the total rate of change of the orientation of the line.

It is also of interest to predict the expected changes in latitude and longitude at a station due to secular motion of the pole. Secular motion of the pole at a rate of a_p and in a direction α_p may be viewed as an angular velocity of the crust with respect to the solid earth [Arur and Mueller, 1971]. In the terrestrial coordinate system, the components of the angular velocity vector of this motion are

$$\Omega_p = \begin{pmatrix} a_p \sin\alpha_p \\ -a_p \cos\alpha_p \\ 0 \end{pmatrix} .$$

As with the angular velocity due to continental drift, the components of this vector may be transformed into a local coordinate system at any station, and the expected rates of change in latitude and longitude, $\dot{\varphi}$ and $\dot{\lambda}$, may be computed. For the numerical predictions, the value of α_p was 285° [Mueller, 1969, p. 82], and the value of a_p was 0".0033 per year [Arur and Mueller, 1971].

The predicted motions at the observing stations for certain types of observations are shown in Figures 20, 21 and 22. Figure 20 shows the predicted rates of change of the length and orientation of selected VLBI baselines.

Although the VLBI's promise to provide the most precise measurement of motion between continents, all stations participating at present in VLBI observations are located on only three of the six tectonic blocks, mostly in America and Europe (unfortunately, a similar statement is true for the lunar ranging stations). The line from Penticton to Parkes, Australia, has the largest predicted rate of change of length. However, a measured change in the length of this baseline would not be a completely satisfactory confirmation of continental drift, since the two stations are not on contiguous tectonic blocks.

Figure 21 depicts the predicted annual rates of change of position due to continental drift and due to secular motion of the pole at selected satellite tracking stations. Most of these stations are participating in the ISAGEX experiment with either Baker-Nunn cameras or laser ranging equipment. However, several proposed stations have been added to provide at least three well separated stations on each of the six tectonic blocks. The proposed stations at Nord, Tromso, Palmer, and Heard Island, are placed at sites previously occupied by BC-4 cameras. Zvenigorod, and Novossibirsk are placed at sites of astronomical observations. Kusai is the site of a former SECOR station. Noril'sk and Kamchatsky are new stations. The values ($d\varphi$, $d\lambda$) written next to the station designations indicate expected changes in the coordinates due to the presently believed rate of secular motion of the pole.

Figure 22 depicts the predicted rates of change of position at selected astronomical observatories. The vectors indicate the expected changes due to the secular polar motion, while the numbers ($d\varphi$, $d\lambda$) written next to the station designations are expected coordinate changes due to continental drift.

2.34 Required Observations.

In order to judge how large a time interval must elapse before changes in position would be detectable, it is necessary to assume certain precisions for each of the observing schedules. The precision with which the VLBI baselines (or the coordinates of lunar ranging stations) will be measured in the next few years is assumed to be 15 cm [Kaula, 1969, p.7-6]. Within a decade, it should be possible to measure the length of the baselines to 2 cm, and to determine their orientation relative to celestial radio sources to 0.001 seconds of arc [Kaula, 1969, p. 7-9, p. 2-1].

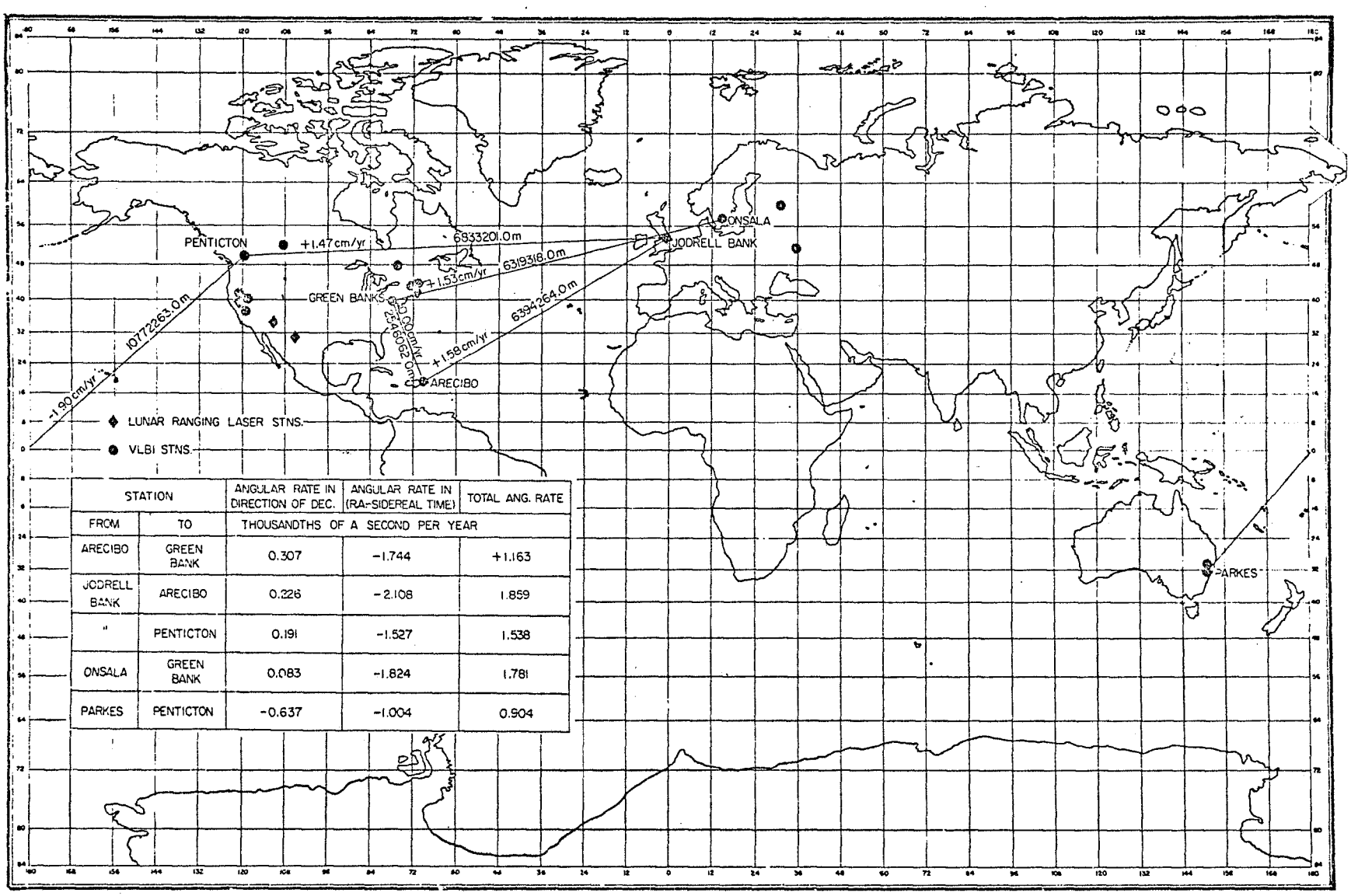

STATION		ANGULAR RATE IN DIRECTION OF DEC.	ANGULAR RATE IN (RA-SIDEREAL TIME)	TOTAL ANG. RATE
FROM	TO	THOUSANDTHS OF A SECOND PER YEAR		
ARECIBO	GREEN BANK	0.307	-1.744	+1.163
JODRELL BANK	ARECIBO	0.226	-2.108	1.859
"	PENTICTON	0.191	-1.527	1.538
ONSALA	GREEN BANK	0.083	-1.824	1.781
PARKES	PENTICTON	-0.637	-1.004	0.904

Figure 20

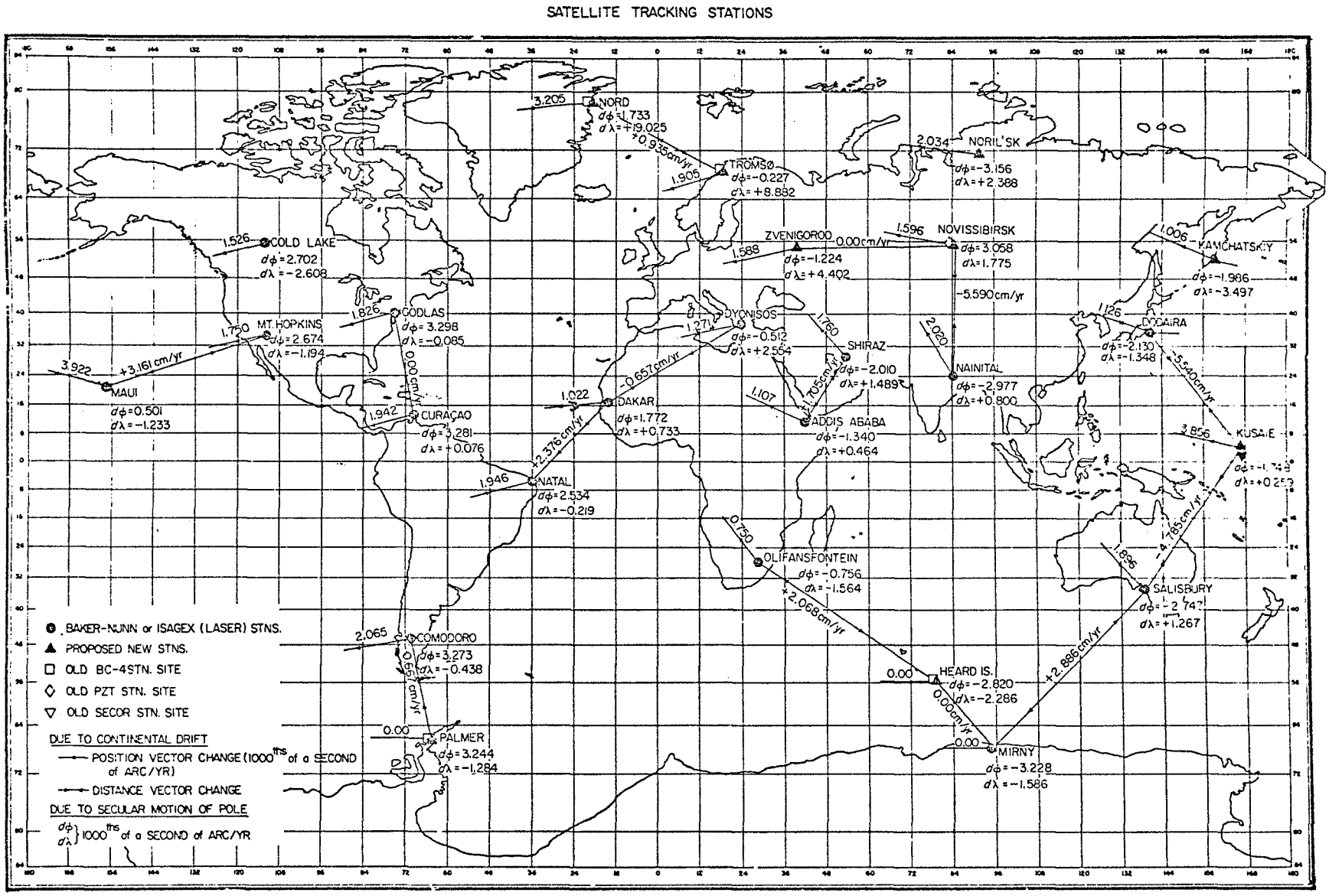
SATELLITE TRACKING STATIONS
NORD
TROMSØ
NORIL'SK
ZVENIGOROD
NOVISSIBIRSK
KAMCHATSKIY
COLD LAKE
MT. HOPKINS
GODLAS
DYONISOS
SHIRAZ
NAINITAL
DYOKIRA
MAUI
CURAÇAO
DAKAR
ADDIS ABABA
KUSAIE
NATAL
OLIFANSFONTEIN
SALISBURY
COMODORO
HEARD IS.
PALMER
MIRNY
BAKER-NUNN or ISAGEX (LASER) STNS.
PROPOSED NEW STNS.
OLD BC-4STN. SITE
OLD PZT STN. SITE
OLD SECOR STN. SITE
DUE TO CONTINENTAL DRIFT
POSITION VECTOR CHANGE (1000ths of a SECOND of ARC/YR)
DISTANCE VECTOR CHANGE
DUE TO SECULAR MOTION OF POLE
1000ths of a SECOND of ARC/YR

Figure 21

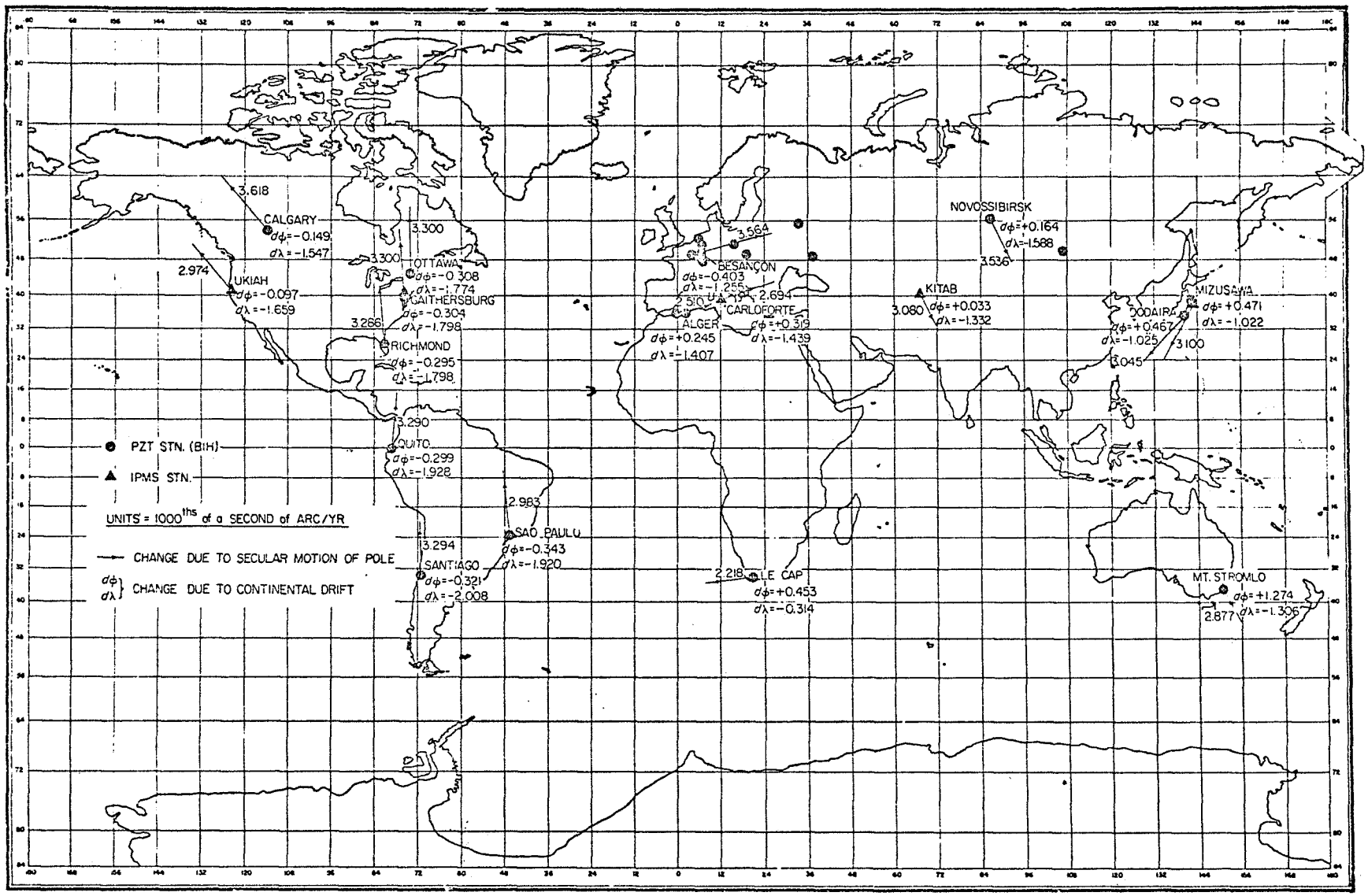
ASTRONOMICAL STATIONS
3.618
CALGARY
dφ=-0.149
dλ=-1.547
3.300
3.300
OTTAWA
dφ=-0.308
dλ=-1.774
GAITHERSBURG
dφ=-0.304
dλ=-1.798
3.286
RICHMOND
dφ=-0.295
dλ=-1.798
2.974
UKIAH
dφ=-0.097
dλ=-1.659
3.290
QUITO
dφ=-0.299
dλ=-1.928
2.983
SAO PAULO
dφ=-0.343
dλ=-1.920
3.294
SANTIAGO
dφ=-0.321
dλ=-2.008
3.664
BESANÇON
dφ=-0.403
dλ=-1.255
2.694
CARLOFORTE
dφ=+0.319
dλ=-1.439
2.510
ALGER
dφ=+0.245
dλ=-1.407
2.218
LE CAP
dφ=+0.453
dλ=-0.314
NOVOSSIBIRSK
dφ=+0.164
dλ=-1.588
3.536
KITAB
dφ=+0.033
dλ=-1.332
3.080
MIZUSAWA
dφ=+0.471
dλ=-1.022
3.100
DOAIRA
dφ=+0.467
dλ=-1.025
3.045
MT. STROMLO
dφ=+1.274
dλ=-1.306
2.877
PZT STN. (BIH)
IPMS STN.
UNITS = 1000ths of a SECOND of ARC/YR
CHANGE DUE TO SECULAR MOTION OF POLE
dφ/dλ CHANGE DUE TO CONTINENTAL DRIFT

Figure 22

The precision of presently operating laser ranging instruments appears to be about one meter. However, ranging precision as high as 15 cm should be achieved within a few years, and a precision of 2 cm should be available within a decade [Kaula, 1969, p.2-9, p. 7-6, p. 7-9]. The precision of optical observations to satellite is in the order of 1".

The precision assumed for observations of latitude and longitude from the astronomical observatories is 0.015 seconds of arc from one night of observations [Mueller, 1969, p. 401]. No improvement in these accuracies is foreseen.

If the motions of the continents and of the pole are really continuous phenomena, then significant changes in the relative and absolute positions of the observing stations should be detectable if the positions are reobserved after a sufficiently long time interval. The time bases in Tables 5 and 6 are computed for the length of time it would take for the predicted motion to equal the uncertainty with which the motion can be observed (1 σ level), and for the length of time required before the existence of motion can be confirmed with a high degree of statistical certainty (3 σ level).

2.35 Conclusions.

Present astronomical and satellite observing stations are not in locations that would be the most advantageous for the detection of relative motions between the continental blocks. Of the lines that are being observed with lasers at both ends as part of the ISAGEX experiment, a rate of change of relative position of more than 2 cm/yr. is predicted only for the line between Dakar and Natal. There is also a line with lasers at both ends between Dodaira and Guam. However, Guam is on the Asian side of the Mariana Trench, which the Le Pichon model considers to be the boundary between the Eurasian and Pacific blocks, and so the model predicts no change in the distance between Dodaira and Guam. If this station were moved to the former SECOR site at Kusai, it would be possible to observe a line between Dodaira and Kusai, where the predicted rate of change is -5.5 cm/yr. The lines between several other pairs of stations, such as Nainatal - Novossibirsk and Salisbury - Kusai, are also expected to change by about 5 cm/yr. If the lengths of these lines are observed to 15 cm within a few years, it should be possible to obtain a strong confirmation of relative motion between continents with a time base of less than a decade.

Table 5

Time Base for Reobservations of VLBI Baselines

From	To	1 σ level	3 σ level
	σ {length} = 15 cm (immediate)		
Arecibo	Green Bank	10 years	30 years
Jodrell Bank	Arecibo	10	30
Jodrell Bank	Penticton	10	30
Onsala	Green Bank	10	30
Parkes	Penticton	8	24
	σ {length} = 2 cm (eventual)		
Arecibo	Green Bank	1.3	4
Jodrell Bank	Arecibo	1.3	4
Jodrell Bank	Penticton	1.3	4
Onsala	Green Bank	1.3	4
Parkes	Penticton	1.1	3
	σ {orientation} = 0".001 (eventual)		
Arecibo	Green Bank	0.8	2.6
Jodrell Bank	Arecibo	0.5	1.6
Jodrell Bank	Penticton	0.7	2.0
Onsala	Green Bank	0.6	1.7
Parkes	Penticton	1.1	3.3

Table 6

Time Bases for Reobservation of Relative Positions Between Satellite Observing Stations

From	To	1 σ level	3 σ level
	σ{distance} = 15 cm (immediate)		
Maui	Mt. Hopkins	5 years	14 years
Dakar	Natal	6	19
Dakar	Dyonisos	23	68
Addis Ababa	Shiraz	9	26
Mirny	Salisbury	5	16
Nord	Tromso	16	48
Kusai	Salisbury	3	9
Kusai	Dodaira	3	8
Nainital	Novossibirsk	3	8

As far as the astronomical observations are concerned, it may be noted from Figure 22 that the expected continental drift will change the coordinates of most observatories mostly in longitude, therefore longitude observations on a continuous basis are of the utmost importance.

Although detection of relative motion between stations on different tectonic blocks is of greatest interest, detection of a lack of relative motion between stations on the same block is of equal importance. The Le Pichon model of global tectonic requires that the blocks be rigid, subject to deformation only at their boundaries. Thus, it is important to determine the extent to which the continents do move as rigid blocks if detection of motion between blocks is to confirm the existence of continental drift. Confirmation of the rigidity of the blocks will require measurements of the relative positions of several additional well placed stations on each block.

2.36 Crustal Movements - Experiments with Secular Polar Motion.

Introduction.

A revised study of the mathematical model as adopted in [Arur and Mueller, 1971] was carried out and it was felt that it would be necessary to modify certain assumptions made therein.

In the previous study only one pole of rotation has been associated in studying the relative motion between American-Eurasian Blocks while referring to Section 2.32 above we should associate instead two poles of rotation, one each for America and Eurasia Blocks (see Table 4).

Assumptions.

The basic mathematical model for secular variation of latitude at any station.

$$-S_i = \omega_j \cos\varphi_j(\sin\lambda_j \cos\lambda_i - \cos\lambda_j \sin\lambda_i) - a(\sin\alpha \sin\lambda_i + \cos\alpha \cos\lambda_i)$$

was retained as such except for the change that a new subscript "j" was introduced to correspond to the angular velocity vector and the polar coordinates of the concerned pole of rotation with respect to the block under consideration, while "i" subscript above refers to the 5 IPMS stations under study. The following values, with their uncertainties, were used in the revised calculations:

(i) for America Block

$$\varphi = 79^\circ.9\ S \pm 8^\circ.8$$

$$\lambda = 40^\circ.4\ E \pm 2^\circ.2$$

(ii) for Eurasia Block

$$\varphi = 62^\circ.9\ S \pm 8^\circ.8$$

$$\lambda = 70^\circ.0\ E \pm 2^\circ.2.$$

Let us associate subscript (3) and (4) with the above poles of rotation, where subscript corresponds to their listing in Table 4.

Calculations.

The revised A and B Matrices used take the form as indicated on pages 56 and 57. The rest of the assumptions and various values were used as earlier and the results obtained are given in Table 7.

A Matrix

$$
\begin{vmatrix}
\omega_3 & \omega_4 & a \\
\cos\varphi_3(\sin\lambda_3\cos\lambda_1 - \cos\lambda_3\sin\lambda_1) & 0 & -(\sin\alpha\sin\lambda_1 + \cos\alpha\cos\lambda_1) \\
\cos\varphi_3(\sin\lambda_3\cos\lambda_2 - \cos\lambda_3\sin\lambda_2) & 0 & -(\sin\alpha\sin\lambda_2 + \cos\alpha\cos\lambda_2) \\
0 & \cos\varphi_4(\sin\lambda_4\cos\lambda_3 - \cos\lambda_4\sin\lambda_3) & -(\sin\alpha\sin\lambda_3 + \cos\alpha\cos\lambda_3) \\
0 & \cos\varphi_4(\sin\lambda_4\cos\lambda_4 - \cos\lambda_4\sin\lambda_4) & -(\sin\alpha\sin\lambda_4 + \cos\alpha\cos\lambda_4) \\
0 & \cos\varphi_4(\sin\lambda_4\cos\lambda_5 - \cos\lambda_4\sin\lambda_5) & -(\sin\alpha\sin\lambda_5 + \cos\alpha\cos\lambda_5)
\end{vmatrix}
$$

where subscripts 1, 2, 3, 4 and 5 refer to the five IPMS stations Ukiah, Gaithersburg, Carloforte, Kitab, and Mizusawa, respectively.

B Matrix

S_1	S_2	S_3	S_4	S_5	φ_3	λ_3	φ_4	λ_4	a
+1	0	0	0	0	$\omega_3 \sin\varphi_3(\cos\lambda_3 \sin\lambda_1 - \sin\lambda_3 \cos\lambda_1)$	$\omega_3 \cos\varphi_3(\sin\lambda_3 \sin\lambda_1 + \cos\lambda_3 \cos\lambda_1)$	0	0	$a(\sin\alpha\cos\lambda_1 - \cos\alpha\sin\lambda_1)$
0	+1	0	0	0	$\omega_3 \sin\varphi_3(\cos\lambda_3 \sin\lambda_2 - \sin\lambda_3 \cos\lambda_2)$	$\omega_3 \cos\varphi_3(\sin\lambda_3 \sin\lambda_2 + \cos\lambda_3 \cos\lambda_2)$	0	0	$a(\sin\alpha\cos\lambda_2 - \cos\alpha\sin\lambda_2)$
0	0	+1	0	0	0	0	$\omega_4 \sin\varphi_4(\cos\lambda_4 \sin\lambda_3 - \sin\lambda_4 \cos\lambda_3)$	$\omega_4 \cos\varphi_4(\sin\lambda_4 \sin\lambda_3 + \cos\lambda_4 \cos\lambda_3)$	$a(\sin\alpha\cos\lambda_3 - \cos\alpha\sin\lambda_3)$
0	0	0	+1	0	0	0	$\omega_4 \sin\varphi_4(\cos\lambda_4 \sin\lambda_4 - \sin\lambda_4 \cos\lambda_4)$	$\omega_4 \cos\varphi_4(\sin\lambda_4 \sin\lambda_4 + \cos\lambda_4 \cos\lambda_4)$	$a(\sin\alpha\cos\lambda_4 - \cos\alpha\sin\lambda_4)$
0	0	0	0	+1	0	0	$\omega_4 \sin\varphi_4(\cos\lambda_4 \sin\lambda_5 - \sin\lambda_4 \cos\lambda_5)$	$\omega_4 \cos\varphi_4(\sin\lambda_4(\sin\lambda_5 + \cos\lambda_4 \cos\lambda_5)$	$a(\sin\alpha\cos\lambda_5 - \cos\alpha\sin\lambda_5)$

Table 7

Result of Analysis

Details of Adjustment Procedure				Results			
Unknowns	Observed Quantities	Constraints	D/F	Values Unknowns 10^{-3} sec/year	Adjusted Values 10^{-3} sec/yr	degrees	V'PV
ω_1, ω_2, a	S_1, S_2, S_3, S_4, S_5	$\varphi_3 = -79.^{\circ}9$ S $\lambda_3 = 40.^{\circ}4$ E for America block $\varphi_4 = -62.^{\circ}9$ S $\lambda_4 = 70.^{\circ}00$ for Eurasia block with zero variance.	2	$\omega_1 = -0.29 \pm 0.01$ $\omega_2 = 0.63 \pm 0.00$ a = 3.25 ± 0.00	$S_1 = 2.15$ $S_2 = 3.20$ $S_3 = 0.63$ $S_4 = -2.54$ $S_5 = -2.89$		0.00
ω_1, ω_2, a	S_1, S_2, S_3, S_4, S_5 $\varphi_3, \lambda_3, \varphi_4, \lambda_4$, α.		2	$\omega_1 = -0.73 \pm 3.8$ $\omega_2 = 0.96 \pm 0.8$ a = 3.43 ± 0.4	$S_1 = 3.09$ $S_2 = 3.01$ $S_3 = -0.05$ $S_4 = -1.76$ $S_5 = -3.25$	$\varphi_3 = -79.9$ S $\lambda_3 = 40.4$ E $\varphi_4 = -62.9$ S $\lambda_4 = 70.0$ E $\alpha = 105.^{\circ}0$ E	0.00
a	S_1, S_2, S_3, S_4, S_5 α	$\omega_1 = 0$ $\omega_2 = 0$ with zero variance.	4	a = 3.67 ± 0.00	$S_1 = 2.89$ $S_2 = 2.66$ $S_3 = 0.30$ $S_4 = -1.55$ $S_5 = -3.47$	$\alpha = 105.0$ E	0.00
ω_1 ω_2	S_1, S_2, S_3, S_4, S_5 $\varphi_3, \lambda_3, \varphi_4, \lambda_4$,	a = 0 with zero variance.	3	$\omega_1 = 22.09 \pm 0.01$ $\omega_2 = 6.10 \pm 0.00$	$S_1 = 4.24$ $S_2 = 2.89$ $S_3 = -1.71$ $S_4 = -4.59$ $S_5 = -3.80$	$\varphi_3 = -79.9$ S $\lambda_3 = 40.4$ E $\varphi_4 = -62.9$ S $\lambda_4 = 70.0$ E	0.00

2.37 References.

Le Pichon, Xavier. (1968). "Sea-Floor Spreading and Continental Drift." Journal of Geophysical Research, Vol. 73, No. 12.

Le Pichon, Xavier. (1970). "Correction to a Paper by Xavier Le Pichon 'Sea-Floor Spreading and Continental Drift.'" Journal of Geophysical Research, Vol. 75, No. 14.

Arur, M. G., and Ivan I. Mueller. (1971). "Latitude Observations and the Detection of Continental Drift." Journal of Geophysical Research, Vol. 76, No. 8.

Mueller, I. I. (1969). Spherical and Practical Astronomy as Applied to Geodesy. Frederick Ungar Publishing Company, New York.

Kaula, William M. (editor). (1969). "Solid Earth and Ocean Physics." Report of a Study at Williamstown, Massachusetts, sponsored by NASA-Electronics Research Center and MIT Measurement Systems Laboratory.

Centre National d'Etudes Spatial. (1971). "International Satellite Geodesy Experiment (ISAGEX) Experiment Plan."

2.4 Investigations Related to the Problem of Improving Existing Triangulation Systems by Means of Satellite Super-Control Points

Program for obtaining the solution vector by Cg-Method using directly A-Matrix was tested on the triangulation chain between Moses Lake and Chandler, for which the originally supplied data was used; this system contains 804 unknowns and 1397 observation equations. This "solution vector program", which has been modified to take care of the ill-conditioning and of minimizing the round-off errors, shows instability of the system as ALPHA - the upper bound of the condition number defined by $\lambda \max/\lambda \min$ - which should be unity for stable systems, is equal to 368 at 2000 iterations for this triangulation chain. This large value of ALPHA could be due to the following reasons:

1) either the configuration of the system is bad,

or 2) the system is undetermined,

or 3) a bad configuration and undetermined system together.

Investigation of the Chain and observed data gave the following results:

a) The Chain contains triangles having unfavorable angles and length-ratios, i.e., angles are as acute as 8° and length-ratio as large as 1:7. Due to this unfavorable configuration, the two points constitute a "double-point" making the system undetermined, causing singularity and bad conditioning.

b) The Chain contains "freely hanging cantilever" figures which hang loosely either within a large figure or run nearly at right angles to the direction of the Chain. Thus, these

have no significant effect on the accuracy of the Chain. However, as these cantilevers are freely hanging, they cause "lack" of observations, making the system undetermined.

To prove the effect of "double-points" and "cantilever" tests were made on a part of the Moses Lake Chain containing 35 stations. The geodetic triangulation data was then screened so as to obtain a well-defined triangulation system, i.e., double-points and cantilevers were removed. The modified geodetic triangulation data (after screening) contain 567 unknowns and 956 equations.

The supplied coordinates of the satellite stations, Moses Lake and Chandler, give some trouble, as use of these yield very large directional L-vectors. Thus, by using these large L-vectors, linearity of the system is lost, which is evident from the results of the solution vector program, which does not yield orthogonal vectors in the first few iterations. The coordinates of these satellite stations need verification.

Covariance Vector Program, which gives one particular column of N^{-1} using Cg-Method, has been accordingly modified for ill-conditioning and for minimizing the round-off errors.

Both programs, namely Solution Vector Program and Covariance Vector Program, have been tested extensively on different systems up to 804 unknowns and 1397 equations. It appears that the number of iterations needed for solution vector depends upon the number of equations besides its dependency upon the number of unknowns, condition of the system and round-off error.

2.5 Investigations Related to C-Band Observations.

The adjustment program OSUGOP uses optical or range observation of Satellite positions to give a least squares adjustment for the observing station positions. It was found necessary to improve the orbital model of the program to permit use of a short arc mode of up to 15 minutes. An orbit integration procedure based on that used by Duane Brown, Inc., in their program SAGA was incorporated into OSUGOP.

Subsequently, the OSUGOP was used to do a number of adjustments of a combined SAO and C-Band network. Three adjustments were carried out in a solution only mode in which the SAO and C-Band data was introduced as weighted constraints.

The SAO data consisted of the station to station directions that were obtained by the SAO's geometric solution. This was a preliminary solution using only optical data of the SAO's Baker-Nunn method which was later combined with dynamic data to obtain the 1969 Smithsonian Standard Earth.

The C-Band data consisted of 6 lengths obtained from the adjustment of the C-Band world-wide network of radar stations observing GEOS-II. Only those lengths were used that could be connected at both eands through first order triangulation to nearby Baker-Nunn stations, thus tying obth networks together.

These adjustments give new solution for the Baker-Nunn stations in which the orientational superiority of the Baker-Nunn optical network was conbined with the accurate range determinations of the C-Band adjustment. The standard deviations of the new solutions showed some improvement over those given for the 1969 Standard Earth and most station positions changed significantly.

As none of these adjustments could take into account the correlation known to exist, especially between the C-Band distances, the resulting

variance-covariance matrices were of questionable value. We then began another adjustment using the SAO optical observations idrectly and combining them with the chosen C-Band lengths introduced, not as constraints, but as observations. This permitted using as weights a full variance-covariance matrix of the pseudo-length observations. This adjustment is still being worked on at this time.

2.6 The North American GEOS-I Tracking Network

The results of the adjustments of the GEOS-I tracking network through the NA-6 adjustment were reported in the Fifth Semiannual Status Report. After the completion of the adjustments through the NA-6, it was very apparent that the weakest of the adjusted station coordinates were the heights. The approximate height coordinates used in the adjustments were taken from the station descriptions on the geodetic data sheets. The only height constraint imposed was at Columbia, Missouri; all others were allowed to adjust freely. At the time, it was not possible to constrain any station heights with any degree of accuracy.

After the completion of all previous adjustments, a new geoid became available from SAO. This geoid gave the heights above the SAO ellipsoid to a very high accuracy. The SAO ellipsoid is earth-centered, and based on comparison of station coordinates in the continental United States, the following shifts were determined for the North American Datum:

$$\Delta x = -38 \text{ m}$$
$$\Delta y = 164 \text{ m}$$
$$\Delta z = 175 \text{ m}$$

The sign convention of these shifts is SAO-NAD.

With the geoid map, it was possible to determine the geoid undulations at each of the observing stations in the optical network. Since the orthometric heights were well determined at the stations, it was simply a matter of adding the geoid height and the orthometric height to arrive at heights with respect to the SAO ellipsoid. By performing a datum transformation the heights were computed with respect to the Clark 1866 ellipsoid.

By using the datum shifts as determined by SAO, and the orthometric heights of the stations, the heights with respect to the NAD were computed.

A comparison with the ellipsoidal heights given on the geodetic data sheets revealed a 33 meter difference in height of the origin station of the network, Columbia, Missouri. There was no agreement anywhere in the network between the given heights and the new computed heights. However, this is to be expected when the origin station has a height discrepancy.

To justify the relative accuracy of the computed heights, the NA-6 solution was readjusted with the new computed height replacing the original NAD heights at Columbia, Missouri. The adjusted heights of all other stations were in very close agreement with the computed heights, verifying the fact that the computed heights were realistic. Therefore, height constraints were placed on all 30 optical stations, using the computed heights and a standard deviation of 5 meters. This was referred to as the NA-8 solution; the results are listed in Table 8.

The NA-8 solution shows the adjusted coordinates to be very realistic, the standard deviations of the adjusted coordinates being smaller than those of any other adjustment. However, it cannot be compared directly with the NAD coordinates because of the height change at the origin. In order to make a comparison with the NAD coordinates, the following shifts must be added to the NA-8 coordinates

$$\Delta x = -1.6 \text{ meters}$$
$$\Delta y = +29.4 \text{ meters}$$
$$\Delta z = -20.5 \text{ meters}$$

These are the shifts of Columbia, Missouri from the NAD coordinates.

Table 8

Coordinates of the North American GEOS-I Tracking Stations from the NA-8 Geometric Adjustment

Station	Name		NA-8	σ
7075	Sudbury, Ontario	X	692,651.9	5.0
	MOTS 40	Y	-4,347,244.3	5.2
		Z	4,600,327.8	4.6
1032	St. Johns,	X	2,602,711.4	69.0
	Newfoundland	Y	-3,419,407.3	82.6
	MOTS 40	Z	4,697,483.9	23.0
3334	Greenville,	X	-84,946.0	5.9
	Mississippi	Y	-5,328,137.9	5.7
	PC-1000	Z	3,493,288.8	6.7
3902	Cheyenne,	X	-1,234,655.7	10.3
	Wyoming	Y	-4,651,395.3	7.8
	PC-1000	Z	4,174,601.5	6.9
1033	College, Alaska	X	-2,299,235.3	14.8
	MOTS 40	Y	-1,445,862.1	40.1
		Z	5,751,645.5	7.6
3400	Colorado Springs,	X	-1,275,164.6	10.5
	Colorado	Y	-4,798,189.8	6.3
	PC-1000	Z	3,994,051.2	6.4
3903	Herndon,	X	1,089,024.2	7.0
	Virginia	Y	-4,843,181.5	4.7
	PC-1000	Z	3,991,553.2	5.2
7039	Bermuda	X	2,308,259.6	7.3
	Island	Y	-4,873,768.5	4.5
	MOTS 40	Z	3,394,403.8	5.1

Station	Name		NA-8	σ
3405	Grand Turk	X	1,919,533.3	6.6
	PC-1000	Y	-5,621,259.5	3.9
		Z	2,315,614.3	7.0
3407	Trinidad	X	2,979,938.0	9.8
	PC-1000	Y	-5,513,709.1	4.8
		Z	1,180,999.5	11.9
3648	Hunter AFB,	X	832,602.0	4.6
	Georgia	Y	-5,349,700.7	2.9
	PC-1000	Z	3,360,426.0	3.8
3404	Swan Island	X	642,530.2	5.3
	PC-1000	Y	-6,054,110.8	4.0
		Z	1,895,536.4	7.2
3657	Aberdeen,	X	1,186,826.5	4.9
	Maryland	Y	-4,785,353.7	4.3
	PC-1000	Z	4,032,731.5	4.0
3406	Curacao	X	2,251,848.0	6.8
	PC-1000	Y	-5,817,084.0	3.7
		Z	1,327,048.4	9.8
7076	Jamaica,	X	1,384,198.3	5.9
	B.W.I.	Y	-5,905,837.1	4.3
	MOTS 40	Z	1,966,390.9	7.7
1021	Blossom Point,	X	1,118,060.3	4.8
	Maryland	Y	-4,876,485.7	3.8
	MOTS 40	Z	3,942,816.1	4.0

Table 8 continued

Station	Name		NA-8	σ
3402	Semmes,	X	167,294.5	4.4
	Alabama	Y	-5,482,137.8	3.3
	PC-1000	Z	3,244,883.8	4.5
3401	L.G.Hanscom Field,	X	1,513,177.0	5.4
	Mass.	Y	-4,463,733.1	5.0
	PC-1000	Z	4,282,902.6	4.0
3106	Antiqua Island	X	2,881,885.5	8.4
	PC-1000	Y	-5,372,339.3	3.8
		Z	1,868,386.6	7.8
3861	Homestead AFB,	X	961,808.8	4.4
	Florida	Y	-5,679,324.0	2.9
	PC-1000	Z	2,729,731.8	4.1
7040	San Juan,	X	2,465,099.4	7.3
	P.R.	Y	-5,535,102.1	3.6
	MOTS40	Z	1,985,359.7	6.9
7043	GSFC,Greenbelt,	X	1,130,748.4	4.7
	Maryland	Y	-4,831,490.0	3.7
	PTH-100	Z	3,993,979.6	3.9
7045	Denver,	X	-1,240,436.8	5.4
	Colorado	Y	-4,760,404.0	3.9
	MOTS40	Z	4,048,826.0	4.1
1042	Rosman, N.C.	X	647,534.9	4.0
	MOTS40	Y	-5,178,101.3	3.0
		Z	3,656,553.1	3.9
7072	Jupiter,Florida	X	976,303.4	4.4
	MOTS40	Y	-5,601,569.2	3.1
		Z	2,880,088.5	4.5

Station	Name		NA-8	σ
7036	Edinburg,	X	-828,460.7	4.4
	Texas	Y	-5,657,636.6	3.3
	MOTS40	Z	2,816,659.3	4.9
1034	E. Grand Fork	X	-521,674.7	3.7
	Minn.	Y	-4,242,224.0	4.4
	MOTS40	Z	4,718,565.8	4.0
1030	Mojave,	X	-2,357,218.4	7.9
	California	Y	-4,646,496.9	4.0
	MOTS40	Z	3,668,147.4	4.1
7037	Columbia,	X	-191,259.0	2.3
	Missouri	Y	-4,967,457.8	2.7
	MOTS40	Z	3,983,105.0	2.9
1022	Ft. Myers,	X	807,890.9	3.9
	Florida	Y	-5,652,159.6	2.7
	MOTS40	Z	2,833,347.1	4.3
5861	Homestead,	X	963,509.5	4.4
	Florida	Y	-5,679,888.6	2.9
	SECOR	Z	2,727,970.8	4.1
5001	Herndon,	X	1,088,884.1	7.0
	Virginia	Y	-4,843,066.3	4.7
	SECOR	Z	3,991,662.7	5.2
5333	Stoneville,	X	-84,964.3	5.9
	Mississippi	Y	-5,328,135.5	5.7
	SECOR	Z	3,493,297.7	6.7
5649	Hunter AFB,	X	832,519.4	4.6
	Georgia	Y	-5,349,740.3	2.9
	SECOR	Z	3,360,381.1	3.8

General Information:

No. of ground stations	34
No. of spatial chord equations	1
No. of degrees of freedom	5254
Quadratic sum of the residuals (V'PV)	5082
Standard deviation of unit weight	1.0

2.7 Computer Programming Efforts.

The only major computer programming effort undertaken was the completion of the new short arc mode geodetic network adjustment program described in the last semi-annual report. No changes were made from that description, and most of the features of the program have now been tested.

The new short arc program combines features from our previous short arc program, from our geometric network adjustment program, and from the SAGA program (written by Duane Brown Associates for AFCRL). The orbit model is based on an expansion of the gravity field into spherical harmonics as far as (4, 4), which is totally adequate for short arc work. The integrations of the orbit and the variational equations are performed in modules taken from the SAGA program, which utilize Taylor's series of 10 terms whose coefficients are developed recursively. If desired, the orbit may be integrated in a coordinate system whose origin does not coincide with the center of mass of the earth, such as the coordinate system defined by a local geodetic datum. A variable length error model for range observations is used. Either a zero set error term or a refraction error term, or both (or neither), may be selected for each station on each pass. The error model is flexible, and each term may or may not be selected on any given pass. All error model terms are subject to a priori constraints. Options are included for a large number of possible weighted or absolute a priori constraints on, and between the station coordinates.

This program is now operational, and test runs have indicated that all of its features operate satisfactorily.

3. PERSONNEL

Ivan I. Mueller, Project Supervisor, part time

Georges Blaha, Research Associate, part time through April 19, 1971

Charles R. Schwarz, Research Associate, part time through March 31, 1971

James P. Reilly, Research Associate, part time

Narendra K. Saxena, Research Associate, full time

Marvin C. Whiting, Research Assistant, part time

Muneendra Kumar, Research Assistant, part time through June 13, 1971

4. TRAVEL

Trips made by project personnel during the report period are:

James P. Reilly
Washington, D.C., March 7 - March 13, 1971
To attend ASP/ACSM Convention and technical sessions

Georges Blaha
Washington, D.C., April 14 - April 15, 1971
To present paper at the American Geophysical Union Meeting and Symposium on Satellite Geodesy

Ivan I. Mueller
Morioka, Japan, May 3 - May 19, 1971
To attend IAU Symposium #48, "Rotation of the Earth" and present paper

5. REPORTS PUBLISHED TO DATE

OSU Department of Geodetic Science Reports published under Grant No. NSR 36-008-003:

70 The Determination and Distribution of Precise Time
by Hans D. Preuss
April, 1966

71 Proposed Optical Network for the National Geodetic Satellite Program
by Ivan I. Mueller
May, 1966

82 Preprocessing Optical Satellite Observations
by Frank D. Hotter
April, 1967

86 Least Squares Adjustment of Satellite Observations for Simultaneous Directions or Ranges, Part 1 of 3: Formulation of Equations
by Edward J. Krakiwsky and Allen J. Pope
September, 1967

87 Least Squares Adjustment of Satellite Observations for Simultaneous Directions or Ranges, Part 2 of 3: Computer Programs
by Edward J. Krakiwsky, George Blaha, Jack M. Ferrier
August, 1968

88 Least Squares Adjustment of Satellite Observations for Simultaneous Directions or Ranges, Part 3 of 3: Subroutines
by Edward J. Krakiwsky, Jack Ferrier, James P. Reilly
December, 1967

93 Data Analysis in Connection with the National Geodetic Satellite Program
by Ivan I. Mueller
November, 1967

OSU Department of Geodetic Science Reports published under Grant No. NGR 36-008-093:

100 Preprocessing Electronic Satellite Observations
by Joseph Gross
March, 1968

106 Comparison of Astrometric and Photogrammetric Plate Reduction Techniques for a Wild BC-4 Camera
by Daniel H. Hornbarger
March, 1968

110 Investigations into the Utilization of Passive Satellite Observational Data
by James P. Veach
June, 1968

114 Sequential Least Squares Adjustment of Satellite Triangulation and Trilateration in Combination with Terrestrial Data
by Edward J. Krakiwsky
October, 1968

118 The Use of Short Arc Orbital Constraints in the Adjustment of Geodetic Satellite Data
by Charles R. Schwarz
December, 1968

125 The North American Datum in View of GEOS I Observations
by Ivan I. Mueller, James P. Reilly, Charles R. Schwarz
June, 1969

139 Analysis of Latitude Observations for Crustal Movements
by M.G. Arur
June, 1970

140 SECOR Observations in the Pacific
by Ivan I. Mueller, James P. Reilly, Charles R. Schwarz, Georges Blaha
August, 1970

147 Gravity Field Refinement by Satellite to Satellite Doppler Tracking
by Charles R. Schwarz
December, 1970

148 Inner Adjustment Constraints with Emphasis on Range Observations
by Georges Blaha
January, 1971

150 Investigations of Critical Configurations for Fundamental Range Networks
by Georges Blaha
(in press)

The following papers were presented at various professional meetings:

"Report on OSU participation in the NGSP"
47th Annual meeting of the AGU, Washington, D. C., April 1966

"Preprocessing Optical Satellite Observational Data"
3rd Meeting of the Western European Satellite Subcommission, IAG, Venice, Italy, May 1967.

"Global Satellite Triangulation and Trilateration"
XIVth General Assembly of the IUGG, Lucerne, Switzerland, September 1967, (Bulletin Geodesique, March 1968).

"Investigations in Connection with the Geometric Analysis of Geodetic Satellite Data"
GEOS Program Review Meeting, Washington, D. C., Dec. 1967.

"Comparison of Photogrammetric and Astrometric Data Reduction Results for the Wild BC-4 Camera"
Conference on Photographic Astrometric Technique, Tampa, Fla., March 1968.

"Geodetic Utilization of Satellite Photography"
7th National Fall Meeting, AGU, San Francisco, Cal., Dec. 1968.

"Analyzing Passive-Satellite Photography for Geodetic Applications"
4th Meeting of the Western European Satellite Subcommission, IAG, Paris, Feb. 1969.

"Sequential Least Squares Adjustment of Satellite Trilateration"
50th Annual Meeting of the AGU, Washington, D. C., April 1969.

"The North American Datum in View of GEOS-I Observations"
8th National Fall Meeting of the AGU, San Francisco, Cal., Dec. 1969 and GEOS-2 Review Meeting, Greenbelt, Md., June 1970 (Bulletin Geodesique, June 1970).

"Experiments with SECOR Observations on GEOS-I"
GEOS-2 Review Meeting, Greenbelt, Md., June 1970.

"Experiments with Wild BC-4 Photographic Plates"
GEOS-2 Review Meeting, Greenbelt, Md., June 1970.

"Experiments with the Use of Orbital Constraints in the Case of Satellite Trails on Wild BC-4 Photographic Plates"
GEOS-2 Review Meeting, Greenbelt, Md., June 1970.

"GEOS-I SECOR Observations in the Pacific (Solution SP-7)"
National Fall Meeting of the American Geophysical Union, San Francisco, California, December 7-10, 1970.

"Investigations of Critical Configurations for Fundamental Range Networks"
Symposium on the Use of Artificial Satellites for Geodesy, Washington, D. C., April 15-17, 1971.

"Gravity Field Refinement by Satellite to Satellite Doppler Tracking"
Symposium on the Use of Artificial Satellites for Geodesy, Washington, D. C., April 15-17, 1971.

"GEOS-I SECOR Observations in the Pacific (Solution SP-7)"
Symposium on the Use of Artificial Satellites for Geodesy, Washington, D. C., April 15-17, 1971.

"Separating the Secular Motion of the Pole from Continental Drift - Where and What to Observe?"
IAU Symposium No. 48, "Rotation of the Earth," Morioka, Japan, May 9-15, 1971.